Université Abou Moumouni

Doctoral Research Program on Climate Change and Energy (DRP-CCE)

NIGER

INTERNATIONAL MASTER PROGRAM

IN RENEWABLE ENERGY AND GREEN HYDROGEN

SPECIALITY: PHOTOVOLTAIC SYSTEMS ANALYSIS FOR GREEN HYDROGEN TECHNOLOGIES

MASTER THESIS

Topic:

OPTIMIZATION OF ACCURATE PV FOR GREEN HYDROGEN PRODUCTION UNDER SAHELIAN CLIMATE CONDICTIONS: CASE OF NIGER

Presented the 25th September, 2023 and by:

Mahoutin Bernard Alexis HONZOUNNON

Jury members

President: Prof. Amadou Seidou Maiga

Examinator: Ass. Prof. Bruno Korgo

German Supervisor: Prof. Dr. Ing. Andrea Benigni

Local Supervisors: Prof. Rabani Adamou **&** Dr. Ayouba M. Abdoulkadri

Academic year 2022-2023

DEDICATION

I would like to dedicate this work to my late father Eloi HONZOUNNON, who left me prematurely without seeing any of my diplomas. Thanks to God and your support, here is a new achievement to make you proud of me.

Dedication to my very dear mother, Beatrice ETCHOU who gave me everything by playing both the role of father and mother in my life.

Lastly but importantly, I dedicate this work to my exceptional wife, who played a key role without whom I wouldn't have achieved this success.

ACKNOWLEDGEMENTS

First of all, I would like to greatly thank God almighty who deserves all honor and glory for helping me complete this master's degree.

I acknowledge with thanks the scholarship and financial support provided by BMBF, The Federal Ministry of Education and Research of Germany and the West African Science Service Centre on Climate Change and Adapted Land Uses (WASCAL) for granting us this master's opportunity.

We also thank the President of the University of Abdou Moumouni for hosting this program.

I would like also to thank the Head of Jülich Forschungszentrum for hosting us for our master's internship.

I would like to thank Pr. Rabani Adamou, the Director of WASCAL DRP-CCE at the University of Abdou Moumouni and my local supervisor for this master's thesis, your support was meaningful and impactful to me.

I extend my appreciation to Ass. Prof. INOUSSA Maman Maarouhi, Coordinator and Deputy Director of WASCAL DRP-CCE at the University of Abdou Moumouni.

I thank also the scientific Coordinator of WASCAL DRP-CCE at the University of Abdou Moumouni, Ass. Prof. MOUNKAILA SALEY Moussa.

I sincerely thank the Coordinator of the IMP-EGH program, WASCAL DRP-CCE at the University of Abdou Moumouni and my Co-supervisor, Dr. AYOUBA MAHAMANE Abdoulkadri for all his support, advice, and encouragement.

I would like to particularly thank my supervisor, Director IEK-10, Forschungszentrum Jülich GmbH, Jülich, Germany, Prof. Dr. Ing. Andrea Benigni for his time, advice and guidance in the completion of this work. You gave a lot to within this short period of my internship.

I can never forget to thank Li Chuan, Ph.D. candidate at IEK-10 Jülich Forschungszentrum who constantly assisted in conducting my master's research by improving my researcher's skills.

I would like to extend my sincere gratitude to all the Jury members for sacrificing your time to examine and appreciate my thesis.

I also have a big thanks to all the staff of this program, in particular, the financial officer, Mr. Hamidou Hama, his assistant and the technical assistant Mr. Agbo David for all your support and the sacrifices you have made to facilitate our stay and study here.

I extend my gratitude to all the lecturers who have educated us through their different courses and advice.

Finally, I would like to thank all my colleagues with whom I shared this wonderful experience and who from now on represent an international and unforgivable family for me.

Abstract

Green Hydrogen has gained significant attention to achieving net zero emissions by 2050 scenario. This study performs an optimization of an Accurate photovoltaic for Green Hydrogen production under severe environment conditions including temperature, wind and dust accumulation effects on photovoltaic modules in the Sahel. Two different photovoltaic models were set up to optimize Green Hydrogen production using COMANDO energy systems modelling framework, an accurate photovoltaic model including the environmental factors mentioned above and a photovoltaic with water-cooling system model that limits the cells overheating and dust accumulation loss. The optimization results of photovoltaic with water-cooling based considering Reversible Solid Oxide Electrolysis Cells, wind turbines, batteries, ground-water suppliers, hydrogen storage, water storage, electricity grid fed in by the electricity excess and a hydrogen demand of 15.3 tons per day revealed better than the results of the accurate photovoltaic with respectively a total annualized investment costs of 88.58 million USD and 84.13 million USD. Similarly, the optimal design of the photovoltaic plant size decreases from 274.22 MWp to 259.78 saving a PV modules installation of 13.13 MWp and 7.5 hectares of land. These results are due to the improvement of photovoltaic operating efficiency by limiting the cells' overheating and dust accumulation through photovoltaic water-cooling. Investigation of the impact of the electrolyzers technologies and the hydrogen demand profile on the optimization results meeting the same daily hydrogen demand shows that hydrogen production using the alkaline electrolyzer with a base demand of 200 kg/h and a pick demand during the daytime up to 2422.6 kg/h gives the best optimization results. The total annualized investment costs dropped significantly from 84.13 million USD to 65.68 million USD led by a significant increase of the photovoltaic size up to 348.22 MWp and a significant decrease in wind turbines from 39.76 MW to 11.54 MW. It can be drawn that Hydrogen production in the Sahel with hybrid solar and wind without battery is more cost-effective in high production during the daytime due to the huge solar potential and lower production on the nights or cloudy days by the wind energy. Finally, it was found that 12,258 m^3 is required for one cooling cycle of 348.22 MWp of photovoltaic plant and this significant amount of water can be used in agriculture to improve food security.

Keywords: Photovoltaic; Green Hydrogen; Optimization; Accurate photovoltaic; Photovoltaic with water-cooling

Résumé

L'hydrogène vert a fait l'objet d'une attention particulière en vue d'atteindre un niveau d'émissions nettes nulles d'ici 2050. Cette étude réalise une optimisation d'un système photovoltaïque fiable pour la production d'hydrogène vert dans des conditions environnementales sévères, y compris les effets de la température, du vent et de l'accumulation de poussière sur les modules photovoltaïques dans le Sahel. Deux modèles photovoltaïques différents ont été mis en place pour optimiser la production d'hydrogène vert en utilisant le cadre de modélisation des systèmes énergétiques COMANDO, un modèle de photovoltaïque fiable incluant les facteurs environnementaux mentionnés ci-dessus et un modèle photovoltaïque avec système de refroidissement par eau qui limite la surchauffe des cellules et la perte due à l'accumulation de poussière. Les résultats de l'optimisation de l'énergie photovoltaïque avec refroidissement par eau basée sur des cellules d'électrolyse à oxyde solide réversible, des éoliennes, des batteries, des fournisseurs d'eau souterraine, un stockage d'hydrogène, un stockage d'eau, un réseau électrique alimenté par l'excédent d'électricité et une demande d'hydrogène de 15,3 tonnes par jour se sont révélés meilleurs que les résultats du modèle du photovoltaïque fiable avec un coût d'investissement total annualisé de 84,13 millions d'USD contre 88,58 millions d'USD. De même, la conception optimale de la taille de la centrale photovoltaïque diminue de 274,22 MWc à 259,78 en économisant une installation de modules PV de 13,13 MWc et 7,5 hectares de superficie du champ. Ces résultats sont dus à l'amélioration de l'efficacité de l'exploitation photovoltaïque en limitant la surchauffe des cellules et l'accumulation de poussière grâce au refroidissement par de l'eau des modules photovoltaïques. L'étude de l'impact de la technologie de l'électrolyseur et du profil de la demande d'hydrogène sur les résultats de l'optimisation répondant à la même demande quotidienne d'hydrogène montre que la production d'hydrogène en utilisant l'électrolyseur alcalin avec une demande de base de 200 kg/h et une demande de pointe pendant la journée jusqu'à 2422,6 kg/h, et en considérant 25 ans de durée de vie des modules donne les meilleurs résultats d'optimisation. Les coûts d'investissement totaux annualisés ont diminué de manière significative, passant de 84,13 millions USD à 65,68 millions USD, grâce à une augmentation significative de la taille de la centrale photovoltaïque, qui atteint 348.22 MWc, et à une diminution significative des éoliennes de 39.76 MW à 11.54 MW. On peut en déduire que la production d'hydrogène dans le Sahel avec un système hybride solaire et éolien sans batterie est plus rentable avec une production élevée pendant la journée en raison de l'énorme potentiel solaire et une production plus faible pendant les

nuits ou les jours nuageux par l'éolien. Enfin, il a été constaté que 12 258 m^3 sont nécessaires pour un cycle de refroidissement d'une centrale photovoltaïque de 348.22 MWc de taille et cette quantité importante d'eau peut être utilisée dans l'agriculture pour améliorer la sécurité alimentaire.

Mots-clés : Photovoltaïque ; Hydrogène vert ; Optimisation ; Photovoltaïque fiable ; Photovoltaïque avec refroidissement par eau

Acronyms and abbreviations

AML:	Algebraic Modeling Languages
APV:	Accurate PV Array
AECs:	Alkaline Electrolysis Cells
CdTe:	Cadmium Telluride
CIS:	Copper Indium Diselenide
CO_2:	Carbon Dioxide
COMANDO:	Component-Oriented Modeling and Optimization for Nonlinear Design and Operation
c-Si:	Crystalline Silicon
DAMFs:	Differential-Algebraic Modeling Frameworks
ECMWF:	European Centre for Medium-Range Weather Forecast
ESMF:	Energy System Modeling Framework
FF:	Fill Factor
FLOSS:	Free Library and Open-Source Software
GHG:	Greenhouse Gas
PROMS:	Process Systems Enterprise
H_2O:	Water Molecule
I:	Direct Current
IEA:	International Energy Agency
IFAD	International Fund for Agricultural Development
I_{max}:	Maximum Output Current
INS	Institut National De La Statistique
IRENA:	International Renewable Energy Agency
I_{sc}:	Short Circuit Current
ITCZ:	Inter Tropical Convergence Zone
$kgCO_2eq/kgH2$:	Kilogram Of CO2 Equivalence Per Kilogram of H2
km	Kilometer
km^2:	Square Kilometer

kWh/m^2:	Kilowatt-Hour Per Square Meter
M KOH:	Mole Potassium Hydroxide
m/s:	Meter Per Second
MAT:	Maximum Allowable Temperature
mc-Si:	Monocrystalline Silicon
min:	Minute
MW:	Megawatt
NOCT:	Nominal Operating Cell Temperature
PCMs:	Phase Change Materials
pc-Si:	Polycrystalline Silicon
PEMECs:	Proton Exchange Membrane Electrolysis Cells
PEM:	Proton Exchange Membrane
P_{max}:	Maximum Power Output
PV:	Photovoltaics
PVC	PV array with Water-Cooling System
Q_h	Heating rate of the Water-cooling system
Q_c	Cooling rate of the Water-cooling system
SOECs:	Reversible Solid Oxide Electrolysis Cells
V:	Voltage
V_{max}:	Maximum Output Voltage
V_{oc}:	Open Circuit Voltage
W/m^2:	Watt Per Square Meter
Wp	Watt peak
ξ_{APV}	Accurate PV plant size
af	Annuity Factor
af	cost per unit of the component
ψ_u	Capital Expenditure
O	Annual Operational Expenditure

List of tables

List of figures

Table of contents

1. Introduction

In recent years, the move towards zero net emissions worldwide has become widely recognized. The Intergovernmental Panel on Climate Change (IPCC) and the international community have shown that climate change is intrinsically linked to anthropogenic emissions, which have already led to a global temperature increase of 1.1°C compared to pre-industrial levels [1]. The energy system, being one of the main contributors to the climate crisis, is responsible for almost 90% of the total carbon dioxide (CO2) emissions and around 75% of the total greenhouse gas (GHG) [2]. Therefore, governments, executives, researchers, and other parties around the world are committed to accelerating the ongoing energy transition and aligning economies with the targets set out in the Paris Agreement to limit global warming to well below 2 °C [3].

According to IEA (International Energy Agency), the net zero emissions will undoubtedly involve a five-fold increase in solar, wind, and other renewable energy sources, and a twofold increase in nuclear energy, thereby reducing the share of fossil-fuel energy from 80 % to 20 % the share of fossil fuels energy based as well [4]. To achieve these goals, hydrogen will be needed to decarbonize energy end uses where other options are less mature or more costly, such as heavy industry, long-haul transport, and seasonal energy storage. In this regard, hydrogen could contribute 10% of the mitigation needed to achieve the IRENA 1.5°C Scenario and 12% of the final energy demand [5]. The growing significance of hydrogen is evident as only one country (Japan) had a national hydrogen strategy in 2017, whereas today, over 30 countries have already developed or are in the process of preparing hydrogen strategies, demonstrating an exponential interest in developing green hydrogen value chains.

Africa is one of the most promising continents, with solar energy accounting for the bulk of its renewable resources. Moreover, its historical experience with earlier generations of electrolyzers dating back to the early 20th century has attracted the attention of international investors, who have now announced several green hydrogen projects. Thus, regions with significant renewable potential will lead as one of the major competitors and key sites for green industrialization [6].

However, despite the enormous solar energy potential and solar PV resources, there are still great challenges in Africa, especially for large-scale PV due to the widespread adoption of the technologies which are not at all due to a scarcity of resources [7]. Financial, human resource,

environmental, and technology challenges are all prevalent. As a result, energy system analysis and energy system optimization could play a key role in some of the challenges mentioned above.

Problem statement

Africa is a continent with a warm climate compared to the northern hemisphere climate. It receives more intense ultraviolet radiation, making it a potentially attractive continent for solar energy deployment.

Indeed, desert countries are best suited to photovoltaic power generation due to the abundant availability of sunlight throughout the year. However, due to the high level of dust and heat conditions, the accumulation of dust particles on the surface of PV modules and the high ambient temperature will negatively affect the reliable performance of the PV array [8]. To overcome these obstacles, the idea of setting up vast solar arrays cooperating with green hydrogen production in Africa and exporting the power to other countries is being addressed. For instance, the Green Climate Fund has announced that it will provide US$150 million in funding to the Desert to Power initiative. This project, led by the African Development Bank and spanning several countries, aims to build 10 GW of PV generation capacity in various projects across the Sahel region to the south of the Sahara Desert[9]. Furthermore, “Power Africa” is an initiative that supports the expansion of Solar Power in West Africa [10]. Recently, the “Africa H_2 Atlas” results for West Africa have revealed enormous potential for producing green hydrogen throughout the Sahelian countries displaying the most attractive potential for both PV and green hydrogen [11]. In 2020, a hydrogen partnership was performed between Germany and Niger. This partnership highlights the potential for Germany and other European countries to opt for the import of green hydrogen as a strategic choice in their efforts to decarbonize the domestic energy supply[12].

All these factors show that numerous ongoing or future solar PV and green hydrogen projects are expected to be implemented. However, existing PV projects reveal that the average daily power loss from dust deposition on solar PV module surfaces is approximately 4.4% over a year. Moreover, there is a decrease in cell operating efficiency by 2% in energy production for every 1°C increase in cell temperature, as observed in an assessment of an installed off-grid PV system [13]. This means that it is crucial to address these issues for the reliable performance of solar PV modules. According to Al-Addous *et al* the financial losses due to dust accumulation can range between 4% and 7% in 2023 for existing solar PV projects [14]. Thus, for large-scale PV solar plants, it is important to employ an optimal workforce and machines to clean the PV panels

regularly. Implementing PV array cooling techniques can minimize the significant losses caused by dust accumulation and temperature variations. Failure to address these concerns may substantially impact the pay-back period and hinder the long-term sustainability of PV projects. Moreover, Al-Addous *et al.* reported in 2019 a 3%–4% reduction in global solar PV power generation even under an optimized cleaning strategy [14]. This reduction in power generation translates to a loss in revenue amounting to 3-5 billion euros, and it is projected to increase further, reaching 7 billion euros by 2023. These findings emphasize the critical need for efficient cleaning and cooling strategies to maintain the economic viability and sustainability of solar PV projects [15].

Currently, the effects of environmental factors on PV power generation, such as ambient temperature, dust accumulation, and wind, have been addressed in various studies worldwide.
To the knowledge of the authors, only a few studies have focused on extreme conditions, and no study has been conducted to develop a model that accurately accounts for PV performance and PV arrays with water cooling systems, specifically considering the unique climate conditions of the Africa countries, such as the Sahel. Such a model is crucial for optimizing green hydrogen production using PV power, especially when considering the practical realities on the ground. Hence, it is necessary to establish an accurate PV array model that incorporates these various losses and also includes a water-cooling system to counteract these effects. By doing so, we can minimize the negative impacts on PV power generation and maximize hydrogen production efficiency. This holistic approach will provide valuable insights into the viability and effectiveness of utilizing PV energy for green hydrogen production in the extreme climate context.

Research questions

Central research question

How to optimize the production of green hydrogen from solar PV systems by considering environmental factors that affect solar PV performance in severe environments?

Research sub-questions

- How do solar irradiation, ambient temperature, wind, and dust accumulation influence the performance of solar PV modules?
- What are the solutions to minimize the negative impact of dust accumulation and solar PV cells overheating on the PV array power output?

- How can we set up two different models where one supplies an accurate solar PV array power output and the second gives an efficient power output considering solar irradiation, temperature, wind, and dust effect?
- What are the optimal cost and designed parameters for hydrogen production using the accurate PV array or the PV array with cooling and what is the best option considering the climate condition of Niger?
- What is the influence of the type of electrolyzer, hydrogen demand profile and PV lifetime on the optimal cost and design parameters for hydrogen production with the cost-effective PV array model under Sahelian climate conditions?

Research hypotheses

- Improving PV array power production using a water-cooling system under Sahelian climate conditions could contribute to efficient green hydrogen production in the Sahel.
- The electrolyzer cost and technology could impact the optimal design and cost of the hydrogen production energy system.

Research objectives

This study aims at:

Optimizing of photovoltaic for green hydrogen production considering the environment factors affecting the PV's performance in the Sahel.

Specific objectives

- Find a mathematical model of solar cell efficiency that includes the parameters of solar irradiation, ambient temperature, and wind;
- Establish the accurate PV array model including the cell efficiency and dust accumulation parameters for getting the accurate operating power output for the installed PV array;
- Set up the model of the solar PV array integrated with water cooling to get the operational PV array power output under cooling conditions;
- Perform the optimization of the energy system for green hydrogen production using each model of solar PV array to draw the best system for green hydrogen;
- Perform a sensitivity analysis with different technologies of electrolyzer, and system configuration.

Structure of the thesis

This study is made up of three main chapters preceded by a general introduction and ends with a conclusion. It is organized as follows: The introduction supplies the necessary background or context for our research problem. Then, the first chapter is the literature review part which aims to retrieve the major findings, limitations, and directions for future research in the scope of our study. Afterward, the second chapter highlights the materials and methods used in this study while the last chapter presents the results and discussion.

Chapter 1

2. Literature Review

2.1. Impact of environmental factors on Solar PV Performance

Solar radiation, ambient temperature, humidity, wind speed, and dust are the most prominent environmental factors affecting photovoltaic systems' performance. Irradiation is the main indicator of solar PV potential, but the other parameters mentioned such as listed above have also a significant impact on the PV module output as PV technology and environmental parameters (wind, temperature, humidity) which allowed us to quantify with precision the amount of electricity produced by a PV system. The PV module manufacturers made the module based on standard conditions of 1000 W/m^2 of irradiance, 25˚C of ambient temperature, air mass of 1.5, and 1 m/s wind speed [16]. These conditions are ideal conditions since during the operation it is subject to real environmental conditions which are dynamic and different from outdoor environmental conditions.

2.2. Impact of solar irradiation

Solar irradiance is the key parameter on a particular site allowing for quantification of the power density of light from the sun or total power from a radiant source reaching a unit area. The Earth receives a constant amount of irradiance through the atmosphere of 1370 W/m^2 [17] while irradiation is the integral of this irradiance over time expressed in kWh/m^2. The irradiation is therefore a principal factor in estimating how much energy is available on a site. The typical solar spectrum falling on the earth's surface without cloud disturbance is approximately 1 kW/m^2 [17]. It has been shown that when all parameters related to the module power output are kept constant the increase in irradiance induces an increase in the power output [18].

Impact of Temperature and Wind

Even though irradiation is the main parameter of PV potential, it is also necessary to consider secondary parameters that influence the PV output. One of the main challenges facing the operation of photovoltaic panels (PV) is the effect of temperature on PV cells since cells' overheating due to excessive solar radiation and high ambient temperature reduces the cells' efficiency [19]. Although the impact of the ambient temperature is not the same for all PV technologies, studies have proved that the impact is not negligible. According to an experimental

investigation in Pakistan done by Perraki *et al.*, it has been reported that, though monocrystalline silicon modules are more efficient than other modules they are more sensitive to temperature [17]. In this regard, a study about the performances of several photovoltaic modules with various technologies: crystalline silicon (c-Si), polycrystalline silicon (pc-Si), Cadmium Telluride (CdTe), and Copper Indium Diselenide (CIS) has been done [20]. He has found that for all c-Si, pc-Si, and CIS modules, the changes in efficiency when modules were running appear to be in the range of absolute 1–2% because of cells' overheating temperature of 30 °C. Moreover, Andreev *et al.* have found through a calculation an increase in photocurrent with the temperature at $0.1\%°C^{-1}$ due to the decreasing of the solar cell gap while the open-circuit voltage decreases at -2 mVC^{-1} within the range of 20°C-100 °C temperature which is not only due to a reduction of the gap but also due to the saturation current increase. It was drawn that these two effects cause a diminution of the maximum available power of 0.35% [21]. In addition to that, it has been shown that heat influences module degradation and long-term exposure to heat will cause the panel to age more rapidly, while some materials may not be able to withstand short peaks of exceedingly hot temperatures [22]. All these findings and the idea to set up a model for cell efficiency that considers the effect of cell temperature led to some models to express the cell temperature. In this regard, several authors have set up models defining cell temperature, some consider the wind parameter while the standard approach is the most known as Markvart's model [23] which does not consider this parameter and just considers the Nominal Operating Cell Temperature (NOCT). Hence, Schwingshackl *et al.* has investigated the effect of wind on solar PV modules. He used five different cell temperature models that were confirmed with experimental results. Those models are the standard approach of Markvart which does not consider the wind and the models of Skoplaki, Koehl, Mattei and Kurtz. The results from this investigation have shown that the wind plays a relevant role in estimating the cell Temperature for most technologies of PV modules [24]. Therefore, the models that include wind as a parameter to estimate the cell temperature have more accuracy even if there is no general model for all the PV technologies. Furthermore, this investigation highlights that the accuracy of the wind data is one important thing that influences the prediction of the cell operating temperature because the results have shown the wind input data for the *in-situ* wind data performs with better results than wind data from the European Centre for Medium-Range Weather Forecast (ECMWF) model. This is an exceptionally good outcome for solar PV array power output prediction since the

proper model for a chosen technology could give cell temperature which is one of the important parameters predicting the PV module output.

2.3. Impact of dust accumulation

Furthermore, Studies have shown in addition to the PV cell overheating, dust accumulation and soiling phenomena are the most affecting PV performance. Hence, several research results discuss the performance of PV modules regarding dust accumulation on the surface. According to Shaharin *et al.*, dust can induce a decrease in peak power by up to 18% for module exposure [25]. Another study [26], done in Egypt has shown 33.5% to 65.8% losses in performance within six months of module exposure. Moreover, Sulaiman *et al.* carried out an interesting study showing power loss due to dust depending on the kind of dust, he used mainly a clean solar module and a module covered with talcum, dust, sand, and moss; it has been noticed for light radiation of 310W/m^2 the power output of the module was reduced by 9%-31%, 60%-70%, and 77%-83% respectively for the modules covered with talcum, dust, sand, and moss [27]. Bonkaney *et al.* carried out dust impact on PV panels in Niamey, dust accumulation has a great impact on the power output of the module [28]. They registered that up to 10% reduction in power has been seen for only 23 days (about 3 and a half weeks). In the same area, Dajuma *et al.* in their study about dust accumulation impact on PV panels in the Sahel, recorded an amount up to 12.46% of power loss after 21 days (about 3 weeks) in September 2015 [29]. Going further, Ndiaye *et al.* investigated the impact of dust deposits on the performance of PV modules by studying the behavior of the open circuit voltage (V_{oc}), short circuit current (I_{sc}), fill factor (FF), maximum output current (I_{max}), maximum output voltage V_{max}, I-V and P-V curves for monocrystalline silicon (mc-Si) and polycrystalline silicon (pc-Si) under one operation year in the Sahel, especially in Dakar. It has been found that dust has a significant impact on Imax, I_{sc}, FF and therefore on the maximum power output (P_{max}). The maximum power output loss ranges from 18% to 78% for respectively for polycrystalline PV and monocrystalline while the I_{max} loss varies from 23% to 80% for respectively for polycrystalline PV and monocrystalline and the fill factor decreases up to 2% and 17% respectively for polycrystalline PV and monocrystalline [30]. We can conclude that the impact on solar PV modules' performance depends on the module's technology. In Sahel, the dust issue is crucial and must be considered while designing PV projects. For all these reasons, incorporating a cooling system into PV modules or PV arrays becomes more relevant for researchers to minimize the cells' overheating phenomenon.

2.4. Solar PV array cleaning and cooling technologies

- **Solar PV cleaning technologies**

There are methods and techniques for the PV modules' surface cleaning for dust effect mitigation on PV power production. However, some technologies like electrostatic cleaning and electrodynamic dust shield methods are not mature and still in development they are therefore not applicable to large-scale PV plants. In 2020, Sheila *et al.* used a conventional cleaning machine that requires water, soap as well and labor to clean a PV module in South Africa with the greatest number of cleanings per year which is the compromise between the cleaning cost and the power loss mitigation due to dust, efficiently to recover 17.7% more power compared with the non-PV array cleaning scenario [31]. Furthermore, In Mali, a Sahelian country, Sidiki *et al.* in 2018, study manually cleaned PV modules using water and soap, cloth, and squeegee to test how effective is this traditional method on PV module's performance. Everyday cleaning was performed between the end of April and the start of June [32]. They recorded a 7% daily average PV power production compared with the no-cleaning case. Moreover, In Nigeria, Chanchangi *et al.*, in 2020 experienced natural cleaning based on rainfall, wind, and gravitational forces due to the PV module/array tilt angle. This method was ineffective during the dry season they made use of manual cleaning which is cheaper after considering labor cost compared with other methods or compared with the power recovered by cleaning [33].

- **Solar PV cooling technologies**

Diverse kinds of cooling systems have already been investigated, there are liquid-based, Air-based, heat pipe-based, and PCM-based (Phase change Materials). Even though the cooling technique depends on several factors such as the PV technology used, PV module geometries as well and climate conditions of the site at which the system is installed, they are classified into two different cooling techniques passive cooling system and active cooling system [34]. Cuce *et al.* has used passive cooling based on phase change materials (PCMs) and found the combination of solar panels and phase change material can allow keeping the panels' temperature under 40 ˚C during 80 min of constant exposure to a radiation of 1000 W/m^2 [35]. Indartono *et al.* has found that the thickness of the PCM greatly affects the cooling efficiency 102 mm PCM thickness gives the best

output power and the efficiency of PV is up to 23.8% and 2.1%, respectively [36]. However, the water-cooling system has revealed better results according to Abdolzadeh *et al.*, efficiency up to 3.26%, 1.40% and 1.35%, respectively are achievable at 16 m head and a mean PV cell efficiency of 12.5% has been achieved during the test day [37]. Moreover, Moharram *et al.* used two new models, heating rate and cooling rate to optimize water-cooling energy consumption [38]. He found that the highest output energy is achieved if PV cooling starts when the temperature of the PV panels reaches a maximum allowable temperature (MAT) of 45 °C. The MAT is the optimized temperature concerning the cooling energy requirement. Therefore, applying optimization techniques in the cooling system will help in figuring out the flow rates at which water should be released to harvest its maximum efficiency simultaneously. Another technique is the micro heat pipe array PV cooling, as air cooling reduces the maximally by 4.7°C the temperature while the output power increases maximally by 8.4%, with an efficiency of 2.6% compared with natural cooling. Water cooling amplifies the cooling in 8°C maximum temperature reduction with an increase in output power up to 13.9% and the efficiency difference is 3%. The maximum efficiency achievable for this technology is 13.5%. After going through several studies in the literature, the water-cooling system is the most attractive to the researchers from a plethora of cooling systems due to the high efficiency and low-cost result that it gives as the optimization tool can help to minimize energy and water consumption for the system, its important added value is water cooling system is the most suitable for hot and dusty climate due to its high efficiency and the dust cleaning effect [39].

Finally, the last method that this study presents is passive cleaning (anti-soiling coatings) which was investigated in Algeria in 2017 by Fathi *et al.* [40], they used the effectiveness of hydrophobic nano-coating on the PV performance due to dust. The result showed an 8% loss in transmission coefficient because of dust accumulation over the coated glass. Another efficient anti-soiling coating method was assessed in 2020 by Alamri *et al.* [41] in Egypt, the authors argued that the technology of cleaning is ineffective in semi-arid climate environments. Addressing all those challenges will impact positively green hydrogen production through water electrolysis technology.

2.5. Green hydrogen production

- **Hydrogen production technologies**

Indeed, several technologies already exist in the past decades before the deployment of modern technologies in distinct stages of development which mostly converge to making hydrogen production environmentally friendly. Based on the named color for each hydrogen-based technology, there is black and brown referring to the gasification of coal the most polluting technology with 20 $kgCO_2eq/kgH_2$ of emissions; and grey hydrogen which is also carbon-intensive and relies on natural gas reforming with associated emissions of 9 $kgCO_2eq/kgH_2$ while blue hydrogen is the grey hydrogen technology with an incorporation of carbon capture and storage with a residual emission in term of long-term plant run. The pink, blue, white, and green hydrogen are clean from CO_2 emissions [42]. Green hydrogen can be produced using water through the electrolysis process, thermolysis, photocatalytic water splitting and thermochemical water splitting while supplying energy from renewable sources including wind, solar, hydro, geothermic and biomass [43].

Indeed, hydrogen production via electrolysis uses renewable electricity and water as the main feedstock and solar and wind play a key role in terms of renewable resources for green hydrogen via electrolysis process because of their widespread and they are expected to drive the enhancement of large-scale green hydrogen production [44]. This technology is aligned with the net-zero emissions target and is known as the most promising and sustainable solution for hydrogen production. According to the IEA, Hydrogen production via electrolysis account currently for 2% of global hydrogen production but the actual water electrolysis hydrogen production momentum has shown a great future development since it is called to replace fossil-fuel-based hydrogen production and to play a key role in the energy transition n production plants mainly autonomous systems using solar energy or wind power, hybrid PV-wind-based systems and grid-connected systems to supply hydrogen for end uses [45]. However, the grid-connected hydrogen is seen as hybrid green and subjected to a constraint of a maximum amount of 4.4 kg CO_2-eq. per kgH_2 annual GHG emissions [46] for keeping its value of greenness according to the certification CertifHy. Thus, the electrolyzer is the main part of whatever system and configuration to get more understanding of the current electrolyzer technologies development.

- **Water electrolysis technologies**

The water electrolysis process is an electrochemical reaction that requires 237.2 kJ mol^{-1} of electricity and 48.6 kJ mol^{-1} of heat to split 1 molecule of H_2O into 2 molecules of hydrogen and 1 molecule of oxygen [47]. Four different water electrolysis technologies are mentioned in the

literature, alkaline water electrolysis, anion exchange membrane (AEM) water electrolysis, proton exchange membrane (PEM) water electrolysis and solid oxide water electrolysis. Indeed, the alkaline electrolyzer is well-established, mature, and commercialized up to the multi-megawatt scale and a global number are successfully deployed for industrial applications [48]. Its electrocatalyst is easily available and low cost with long-term stability for H_2 production. However, it has limited current densities, low gas purity as well as a lower operating current density, cell efficiency, and crossover. Regarding AEM, it is the latest technology, that is to overcome the drawbacks of alka98line and PEM water electrolysis. It has metal-free electrocatalysts as well as low-concentrated (1M KOH) liquid electrolytes. However, its limited stability and low level of development hamper its deployment [48]. PEM water electrolysis gives several advantages over alkaline in terms of high operating current density, high purity of gases, higher outlet pressure, and smaller footprint while the major challenge is the cost of their components mainly its electrocatalysts. It is the second mature and commercially available technology that is scaling up to megawatt (MW) for industrial and transportation. Solid oxide water electrolysis technology is still developing while reaching the commercialization stage. The great advantage is the high efficiency achievable and the feverish temperature working principle (700-850°C). However, it has been noted that it has limited stability and a long starting time [48].

2.6. Energy system optimization

Energy system optimization is a tool used for achieving the best possible result under given conditions. In other words, the optimization problem is made up of three main parameters needed objective's function, a set of unknowns or variables and the constraints. Many optimization techniques have been found in the past three decades to improve the operation and control of energy systems aiming at either minimizing efforts or maximizing profit [49].

Currently, research in energy systems optimization is more focused on different energy systems within various integrated ranges. This optimization can be broken down into design, synthesis, and operation, as well as different static and dynamic problems followed by the solutions as detailed by Frangopoulos [50]. However, some parameters like energy demands, prices, weather, and other operational aspects can be strongly varying over time making therefore, their future values highly uncertain, which renders the design and operation of energy systems more challenging when decisions should be processed. Amer *et al.* [51]in 2013 from the study they

carried out proposed hybrid system optimization models of various renewable energy sources to minimize the total cost of Renewable energy systems.

Chapter 2

3. Materials and Methods

3.1. Study area

3.1.1. Description of the selected region:

The region of our study is the Sahel precisely Niger which has a surface area of 1,267,000 square kilometers (km^2), bordering Mali, Burkina Faso and Benin to the Western part, Nigeria to the Southern, Chad to the Eastern and Algeria and Libya to the Northern part. Niger is subdivided into eight regions with 36 provinces and 265 districts. It has a long river of 550 km (about the length of New York State) in length. Niger's population is 16 million with an annual growth rate of 3.3% with a population density of 12 people per km^2 according to the ''Institut National de la Statistique (INS), 2012'' [52]. For this study of optimization, the climate input data concern a specific position located in Agadez with the geographical coordinates: Longitude 7.9628 and latitude 16.9522 (**Figure 1**).

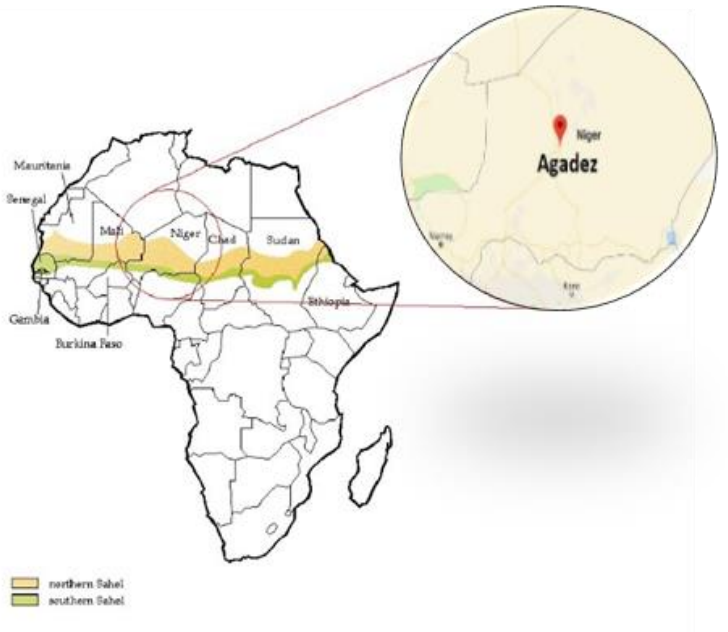

Figure 1*: Sahel, Niger map and Agadez location*

3.1.2. Climate Characteristics of the study area

Being one and even the central region of the Sahel, Niger's climate is one of the hottest semi-arid climates within the Sahel specifically characterized by a single and short annual rainy season of about 3-4 months (June, July, August, and September) and dry season from October to May associated with the Northward movement of the Inter Tropical Convergence Zone (ITCZ). The Harmattan is a strong dry and dust wind characterized by the cold season which usually starts from November to the end of February. Niger has an untapped renewable energy potential especially solar and wind which provides opportunities for transforming urban and rural livelihoods and producing competitive hydrogen in the world.

3.1.3. Solar and wind potential of the study area

Niger enjoys high solar radiation conditions in all eight of its regions. Average solar radiation is 5-7 kWh/m^2 per day, and there are seven to ten hours of sunshine per day on average. April to August is the period of high insolation when the diurnal variation between minimum and maximum radiation values is small. The rainy season coincides with the high solar radiation summer months. Arlit and Agadez cities in the northern and central regions respectively and Niamey and Zinder in the southern solar data recorded confirm the enormous potential of PV more specifically in those

regions. Referring to the wind potential, the study concluded, that Niger has an average wind of 2-6 m/s at the height of 10m while increasing in height amplifying the wind speed [52].

3.2. Materials

The materials needed to perform the study of optimization model for green hydrogen production based on solar PV as the main electricity source and wind power as the second electricity source for the water electrolysis process are software with an energy system modeling framework since it is a simulation.

3.2.1. Python software

Python is an object-oriented programming language created by Guido Rossum in 1989. It is ideally designed for rapid prototyping of complex applications. It has interfaces to many OS system calls and libraries and is extensible to C or C++ with the possibility of embedding it with C/C++ programs to give 'scripting' capabilities for your program's users. Hence, it is the software within which the Energy System Modeling Framework is installed and also the software that was used to perform the PV accurate model and the PV with cooling model to get their respective outputs that constitute one of the key input data used for the optimization.

3.2.2. COMANDO Energy Systems Modelling Framework

COMANDO is defined as Component-Oriented Modeling and Optimization for Nonlinear Design and Operation (COMANDO) open-source Python package (COMANDO Repository). It is a new tool that was developed in 2021 by Langiu *et al.* [53] in Forschungszentrum Jülich and RWTH Aachen University and proposed to address the challenges of technical design and operation. COMANDO borrows a generic, nonlinear representation of mathematical expressions and features for algorithm development from AMLs (algebraic modeling languages), and the representation of differential equations and more general system model aggregation from differential-algebraic modeling frameworks (DAMFs) such as PROMS (Process Systems Enterprise, 1997-2019), MODELICA (Elmqvist and Mattsson, 1997), or DAE Tools (Nikolić, 2016). With this combination of features, COMANDO incorporates flexible nonlinear and dynamic modeling into the modularity

of an ESMF (energy system modeling framework). Additionally, COMANDO enables the simultaneous consideration of multiple operating scenarios through a two-stage stochastic programming formulation, allowing for rigorous optimization of energy system design and operation under uncertainty and/or variability of operating conditions. While the vast majority of existing ESMFs (energy system modeling frameworks) are implemented as a layer on top of an AML (algebraic modeling languages), COMANDO is based on the computer algebra system SymPy [54]. SymPy provides data structures for representing generic mathematical expressions and corresponding methods to analyze and manipulate expressions. These features facilitate the creation of automatic reformulation routines (e.g., automatic linearization), custom interfaces to AMLs or solvers, and user-defined solution algorithms. Finally, COMANDO is a tool that allows for flexible model creation regardless of the capabilities of existing MILP-based energy-system modeling tools by providing a wide range of options for problem formulation. Contrary to classical algebraic modeling frameworks, it allows for modular component and system representations and is dedicated to energy system design and operation.

3.3. Methods

The energy system models of this study are focused on hydrogen production by solar photovoltaic and wind turbines, the elements and components for different conversion processes. The renewable energy sources solar and wind are two different technologies of production of solar and wind primary energy sources into electricity within the energy system. Besides, three different storage mediums batteries, hydrogen storage tanks and water reservoirs intend to store the excess of electricity, hydrogen produced and water pumped respectively. An electrolyzer within the system produces hydrogen thanks to the electricity and water supply for the electrolysis process. Therefore, it is paramount to start the optimization model of this study which is highly relied on uncertain electricity availability due to the intermittency of the energy sources. Hence, after setting up all the components required for the energy system creating the energy system and the energy system components connections. The problem formulation is followed to get the optimized size of every design parameter and the system's objective costs via an optimization problem solver. Finally, the optimization model of this work aims to study the optimal schemes under extreme conditions that can make the most effective use of resources considering the investment costs of system components and the environmental factors affecting the PV power supply. This will help to achieve the best solution under the environmental constraints for any location in a severe climate

environment. This can subsequently help the stakeholders to make investment decisions for green hydrogen production.

Figure 2 presents the flowchart of the optimization method.

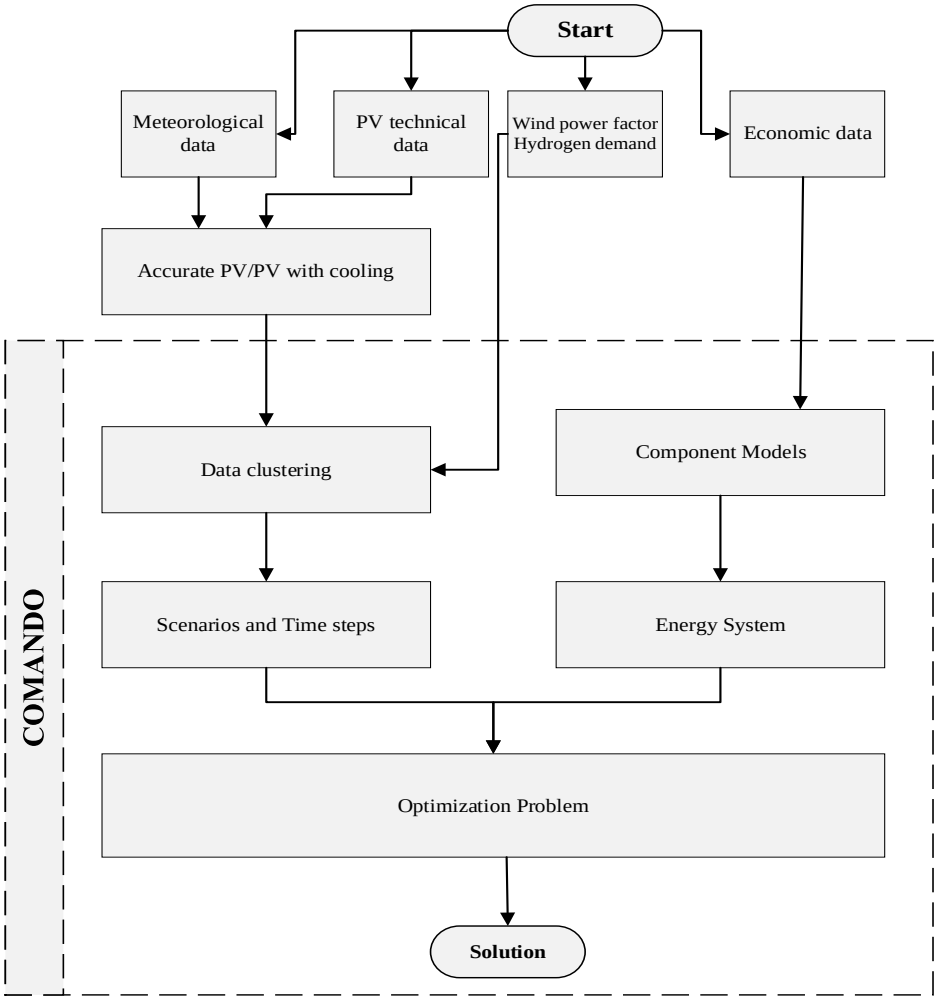

Figure 2: *Energy System Optimization flowchart*

3.3.1. Modelling

- **Component Models**

The components of the energy system are an Accurate PV array, a Cooling PV array (PVC), wind turbines; three different electrolysis technologies (Reversible Solid Oxide Electrolysis Cells, Alkaline electrolysis Cells and Proton Exchange Electrolysis Cells) to produce hydrogen, batteries for electricity storage and hydrogen storage to store hydrogen; ground water supplier, water storage, a wastewater collector from the PVC, electricity grid and hydrogen demand. Within the

COMANDO energy systems modeling framework, a class component should be imported before starting the development of the model of each component.

- **Solar accurate PV Model**

The solar-accurate PV model aims to represent almost a real PV power supplier within the energy system. This model contains a sub-model that includes the cell temperature, the wind and the dust, the most relevant factors affecting the theoretical or expected power output from a designed PV array. Those parameters mostly are neglected while designing PV solar plants by considering only the irradiation or using the PV factor from open-data sources (Renewable ninja) based on the western reality [55]. The accurate PV array (APV) model is made up of a main input parameter which is the PV power per square meter (kW/m^2), this input data derives from the result of a mathematical model which requires solar irradiance, wind speed at 10 meters, ambient temperature, dust accumulation loss and the module's efficiency. Then, follow a design parameter which is the size needed to be installed (km^2), an operational variable that defines the operating PV power output with an output connector, the constraints and the cost expressions.

- **Accurate PV power output model**

The cell temperature expresses the operating temperature of the solar cell and is established by Sandia who considers the ambient temperature, wind speed and solar irradiance as parameters driving the cell temperature [55].

$$T_c = \phi[e^{a+b*W_s}] + T_a + \frac{\phi}{\phi_o} * \Delta T \qquad 3.1$$

Where**,** T_c is the cell operating temperature (°C), T_a is the ambient temperature (°C), ϕ is solar irradiance incident on module surface, (W/m^2), W_s is wind speed (m/s) measured at standard 10m height, a is an empirically-determined coefficient establishing the upper limit for module temperature at low wind speeds and high solar irradiance, b is also an empirically-determined coefficient establishing the rate at which module temperature drops as wind speed increases, ϕ_o is the reference solar irradiance on module, (1000 W/m^2) and ΔT is the temperature difference between the cell and the module back surface at an irradiance level of 1000 W/m^2. This temperature difference is typically 2 to 3 °C for flat-plate modules in an open-rack mount.

The cell efficiency is then expressed based on the cell temperature and the efficiency of the module at the Standard Test Conditions (STC) [56].

$$\eta_{op} = \eta_r[1 - \beta_r(T_c - T_r)] + \gamma \text{ Log } (\phi) \quad 3.2$$

Where η_r stands for the reference (STC) module efficiency, β (%°C $^{-1}$) and γ are respectively the solar irradiance and temperature coefficient for the PV module. The cell's reference temperature T_r equals, 25°C and the reference solar irradiance ϕ is $1000\ Wm^{-2}$ It has been noted that the parameters T_r , η_r , β and γ are provided by the PV module manufacturer.

PV power output at STC is the following equation [38]:

$$P_r = \eta_r * A * \phi \quad 3.3$$

A is the unit area (m^2) and P_r the power peak at STC.

The APV power output during operation at any instantaneous time can be obtained by substituting η_r by η_{op} in equation 3.3. Then, the APV power output per square meter considering solar irradiance and wind is as follows:

$$P_{op} = \eta_{op} * A * \phi \quad 3.3$$

Finally, the dust accumulation and soiling loss (η_{loss}) is introduced into equation 3.4 to get the final expression of the APV power output per unit area (W/m^2)

$$P_{opAPV} = \eta_{op} * A * \phi\ (1 - \eta_{loss}) \quad 3.4$$

P_{opAPV} is APV operating power output and η_{loss} is dust and soiling loss.

- **Component model constraint**

The constraints set in the APV model are as follows:

$$E_{out} \leq P_{opAPV} * \xi_{APV} \quad 3.5$$

Where E_{out} is the electricity per unit of time generated by the APV and $\xi_{APV}$is the size need to be installed.

- **General cost functions for all the component models**

The cost functions are general for all the component models and their equations are as follows [57] :

$$af = \frac{\mathrm{i} * (1+\mathrm{i})^{\mathrm{n}}}{(1+\mathrm{i})^{\mathrm{n}} - 1} \quad 3.6$$

n is the component lifetime, i: interest rate and af is the annuity factor.

$$\mathrm{K} = af * \psi_u * \xi \quad 3.7$$

K is the capital expenditure, ψ_u is the cost per unit of the component and ξ is the installed size of the component.

$$\mathrm{O} = \mathrm{K} * \delta \quad 3.8$$

O is annual operational expenditure and δ is the fraction of K allocated for operation and maintenance.

- **Solar PV with cooling system Model**

Setting a PV array model with a water-cooling (PVC) system aims to improve the efficiency of the PV array power output by mitigating temperature and dust or soiling accumulation on PV module performance. Water-cooling was chosen because of the significant efficiency achievable with this technology, and the environmental conditions of the study area. Therefore, a water-cooling model is integrated into the PV array to maintain the module temperature at a maximum allowable temperature (MAT) of 40℃. The MAT is a compromise value between the cooling energy and water consumption giving the best performance the cooling can start. So, the cooling system made up of a water pumping system should start working and cool down the PV array till a certain temperature below the MAT before stopping. As this study is dealing with hourly time steps data, the cooling time is assumed to be based on hourly time steps.

Indeed, our study area is an area of surface water scarcity but is rich in ground water. Its availability has been proved by a study financed by the Millennium Challenge Corporation (MCC) that found that Niger is the most groundwater-rich country in the Sahel region. So, tapping into its abundant groundwater resources, Niger can potentially increase its irrigation capacity across an area of over 2 million hectares of arable land overlying these aquifer systems [58] and Agadez is part of the richest regions within the country. Hence, the idea is pumping water from the ground to cool down the PV array and then, collecting the wastewater from the PV array that will be channeled to supply water for agricultural purposes makes it relevant.

Furthermore, an optimization of the power out from the PVC will be performed to ensure its effectiveness concerning the APV. This means that the cooling system working principle is not only based on the MAT but depends also on the PV power output gap between the PVC and APV, it

should be greater or equal to the energy requirement for the cooling system for the cooling activation. Therefore, the PVC will never produce energy less than the APV if it has been installed in place as the power output of the PV array is more valuable than the wastewater for Agriculture. The model configuration of PVC is similar to the APV except for the cooling system added. It is comprised of the solar power output per unit area as the main input data parameter which results from mathematical models of the cells operating efficiency in function of the cell temperature, solar irradiance, and the MAT. Then, the design variable is the size (km^2 or MWp) followed by two operational variables, one is the operating power output having an output connector and the second is the wastewater flow after cooling which is connected to an output connector, the constraints and cost expressions (equations 3.6, 3.7 and 3.8).

- **Power output model**

Here, the MAT is assumed to be the module/array temperature and by replacing T_m expression in equation 3.1 gives the cell temperature (T_{cc}) equation 3.9, afterwards the T_{cc} is introduce in equation 3.2 to get the cell operating efficiency (η_{opc}) and finally, the latter is introduced by substitution of η_r by η_{opc} in equation 3.3 giving the power output of the PVC (P_{opc}). This leads to the following equations:

$$MAT = T_m = \phi[e^{a+b*W_s}] + T_a \qquad 3.9$$

$$T_{cc} = MAT + \frac{\phi}{\phi_o} * \Delta T \qquad 3.10$$

$$\eta_{opc} = \eta_r[1 - \beta_r(T_{cc} - T_r) + \gamma \text{ Log } (\phi) \qquad 3.11$$

$$P_{opc} = \eta_{opc} * A * \phi \qquad 3.12$$

- **Power output model optimization equation**

$$Ppump = \rho * g * Q * TDH / \eta(motor\text{-}pump) \qquad 3.13$$

$$P_C(x) = \begin{cases} P_{op} \ , & \text{Ppump} - x < 0 \\ P_{opc} - \text{Ppump}, & \text{Ppump} - x \geq 0 \end{cases} \qquad 3.14$$

$Ppump$ is the pumping power; ρ is the water density; Q is Water flow rate per hour for cooling $1m^2$ of PV array; *TDH* is the Total Dynamic Head of the pumping system and $\eta(motor\text{-}pump)$ is the efficiency of the motor-pump; P_{opc} is the power output of PV during cooling times.

$P_C(x)$ is the optimized power output of the PVC, $x = P_{opc} - P_{op}$ is power gap gained by cooling, Ppump is cooling power requirement and P_{op} is the optimal power output when the power gap is less than 0. In another word, the PVC behaves like the APV and provides the APV's power output for this particular time.

- **Cooling system parameters equation**

The mathematical model used to evaluate the cooling system includes the cooling rate (Q_C) and the heating rate (Q_H) of the module. Equations 3.15 and 3.18 express respectively the heating rate and the cooling rate [38].

Indeed, the cooling rate can be determined based on an energy balance equation 3.16, such that the heat energy gained by cooling water is equal to the heat energy dissipated from the PV panels by assimilating the PV module's glass temperature as the module temperature the change in temperature of the modules is the change in temperature of the module's glass.

$$Q_h = \frac{\Delta T_m}{\Delta t} \qquad 3.15$$

$$Q_{gained\ by\ cooling\ water} = Q_{dissipated\ from\ PV\ modules} \qquad 3.16$$

$$\dot{m}_w * t_c * C_w * \Delta T_w = m_g * C_g * \Delta T_g \qquad 3.17$$

$$Q_c = \frac{\rho_w \dot{V}_w * C_w * \Delta T_w}{t_c * \rho_g * A_g * X_g * C_g} \qquad 3.18$$

With $m_g = \rho_g * A_g * X_g$ and $\dot{m}_w = \rho_w * \dot{V}_w$; ρ_g is the density of tempered glass, $\rho_w \dot{V}_w$ is mass flow rate of water, C_g is the heat capacity of glass, C_w is the specific heat capacity of water; ΔT_g is the glass temperature changes due to water cooling, ΔT_w is the water temperature rise, A_g is the surface area of the PV module/Array, X_g is the thickness of the glass covering the PV panel and $t_{cooling}$ is the time taken to cool the solar PV panel to a moderate optimally the modules' temperature with respect to MAT, Δt the heating time of the module and ΔT_m is the temperature increase with respect to Δt. The mass flow rate of water is set for a value of 7.2 liters per hour for considering $1m^2$ of cooling area accordingly the study done by Basrawi *et al* [59] in 2020.

This study is most focused on the energy system optimization however the aforementioned-parameters will be calculated for a day to examine the performance of the cooling system.

- **Component model constraint**

$$E_{outPVC} \leq P_C(x) * \xi_{PVC} \quad 3.19$$

Where E_{outPVC} is the electricity per unit of time generated by the PVC and ξ_{PVC} is the size need to be installed.

$$\omega = \xi * \dot{V} * t_c \quad 3.20$$

ω is the water collected after cooling, $\dot{V}$ is the water flow rate and, t_c is the cooling time, for one cycle cooling is equals to 1h.

- **Wind turbine power plant Model**

Wind power is the second energy source of the energy system that is intended to be set. Hybrid solar and wind give better optimization results than only PV energy systems if the area is a promising area for wind energy. Agadez is an area both windy and sunny.

The wind turbine model is comprised of an input parameter which is the wind power factor, a design parameter that aims to provide the optimal size (MW) after optimization, an operational parameter which is the electricity output generated by the turbines which is linked to an output connector, the constraints and the cost expressions.

- **Component model equations**

$$E_{Tur} \leq \tau * \xi_{Tur} \quad 3.21$$

E_{Tur} is wind turbines electricity output, τ is the wind power factor and ξ_{Tur} is the wind farm size.

- **Electrolyzer Models**

The electrolyzer is one of the key components of the energy system to be set up. Hence, after reviewing the technologies of electrolyzers available, this study intends to use the technologies of Solid Oxide Electrolysis Cells (SOECs) as baseline, followed the Alkaline Electrolysis Cells

(AECs) and lastly the Proton Exchange Membrane Electrolysis Cells (PEMECs) for the sensitivity analysis.

- **Reversible Solid Oxide Electrolysis Cells (RSOECs)**

SOECs are one of the most efficient water electrolysis technologies although it is still in the development process. Due to its reversibility working mode, the same stack of the RSOECs can run as a fuel cell or electrolyzer. This feature was included within the RSOECs model giving option of inputting electricity into the energy system. RSOECs' model is made up of a design parameter that is the size or capacity needed to be installed (MW) while operating as an electrolyzer, it has an operational variable for the electricity input having an input connector, a second operational variable for the hydrogen output when performing as electrolyzer with an output connector, and the third operational variable which is the water input having an input connector. While running as a fuel cell, it has an operational variable for the hydrogen input with an input connector, a second operational variable controlling the electricity output with an output connector and the cost expressions (equations 3.6, 3.7 and 3.8).

- **RSOECs model equations**

Since the RSOECs perform whether as Solid Oxide Electrolysis Cells (SOECs) or Solid Oxide Fuel Cells (SOFCs) it is connected to three buses (Hydrogen bus, water bus, electricity bus) the node (bus) is always balanced between the commodity input and output so the RSOECs can never perform its two modes at the same time. The equations established in the model are:

$$E_{SOECs} \leq \xi_{RSOEC} \qquad 3.22$$

$$H_{2out} = (E_{SOECs} * \eta_{RSOECs})/LHV_{H_2} \qquad 3.23$$

$$\omega_{in} = 0.0126 * H_{2out} \qquad 3.24$$

$$E_{SOFCs} = (H_{2in} * \eta_{RSOECs}) * LHV_{H_2} \qquad 3.25$$

$$H_{2in} \leq \xi_{RSOECs}/LHV_{H_2} \qquad 3.26$$

E_{SOECs} is the SOECs electricity input, ξ_{RSOEC} is the RSOECs optimal the size need to installed, H_{2out} is the Hydrogen output of SOECs, ω_{in} is the water input to the SOECs, 12.6 kg of ground water is required to produce 1 kg of hydrogen [60], LHV_{H_2} is the low heating value of hydrogen, E_{SOFCs} is the electricity output of the SOFCs and H_{2in} is the hydrogen input to the SOFCs.

- **Alkaline Electrolysis Cells (AECs) and Proton Exchange Membrane Electrolysis Cells (PEMECs)**

The AECs and PEMECs have the same model configuration. They differ from the input data (Cost, efficiency, and lifetime). Hence, the same constraints are applicable for both of them. This model is characterized by a design parameter which is the size of the electrolyzer (MW), an operational parameter for the electricity input (with input connector) and the second operational parameter for the hydrogen output (with output connector) and the third operational variable for water input (with input connector) as well as the cost expressions (equations 3.6, 3.7 and 3.8).

- **AECs/PEMECs model equations**

$$E_{El} \leq \xi_{El} \quad 3.27$$

$$H_{2Elout} = (E_{El} * \eta_{El})/LHV_{H_2} \quad 3.28$$

$$\omega_{in} = 0.0126 * H_{2Elout} \quad 3.29$$

E_{El} is the electrolyzer (AECs or PEMECs) electricity input, ξ_{El} is the optimal size of the electrolyzer, η_{El} is the efficiency of the electrolyzer and H_{2Elout} is the Hydrogen output of the electrolyzer.

- **Electrical Battery, Hydrogen storage and Water storage models**

The electrical battery, hydrogen storage medium and water storage are the three storage means of the energy system. Their models are quite similar apart from the fact that while the battery stores electricity from solar or wind, the hydrogen storage stores hydrogen (energy carrier) from the electrolyzer and the water storage stores water to supply it to the electrolyzer later. Hence, the battery has a design parameter which is the size of the battery pack (MW), an electricity input operational variable (with an input connector), an electricity output operational variable (with an output connector) and the battery state of charge operational variable. Similarly, the hydrogen

storage model disposes of a design parameter which is its optimal size (kg), a hydrogen input operational variable (with an input connector), a hydrogen output operational variable (with an output connector) and the hydrogen storage state of charge operational variable. For the water storage, it also follows the same model conjugation, the design parameter for the water storage size (m^3), then, the operational variable for the water input (with input connector) and the operational variable for water output of water storage (with output connector). They all have the same cost expressions mentioned in equations 3.6, 3.7 and 3.8.

- **Battery, hydrogen storage and water storage model constraints**

Battery

$$\varsigma_d = \varepsilon_{bat} * \eta_{loss} \quad 3.30$$

$$\varepsilon_{bat} \leq \xi_{bat} \quad 3.31$$

$$\varepsilon_{bat} = E_{in} * \eta_{char} - E_{out} * \eta_{dis} \quad 3.32$$

$$3.33$$

ς_d is the battery self-discharge, $\varepsilon_{bat}$is the battery state of charge, η_{loss} is the capacity losses, ξ_{bat} optimal size of the battery, E_{in} is the electricity input and E_{out} is the electricity output of the battery. η_{char} is the charging efficiency and η_{dis} is the discharging efficiency.

Hydrogen storage

$$\varsigma_{H_2} = \varepsilon_{H_2} * \eta_{H_2} \quad 3.34$$

$$\varepsilon_{H_2} \leq \xi_{H_2} \quad 3.35$$

$$\varepsilon_{H_2} = H_{2_{in}} * \eta_{charH_2} - H_{2_{out}} * \eta_{disH_2} \quad 3.36$$

ς_{H_2} is the hydrogen self-discharge, $\varepsilon_{H_2}$is the hydrogen storage state of charge, η_{H_2} is the capacity losses due to leakage, ξ_{H_2} optimal size of hydrogen storage, $H_{2_{in}}$ is the hydrogen input and $H_{2_{out}}$ is the hydrogen output of the hydrogen storage. η_{charH_2} is the charging efficiency and η_{disH_2} is the discharging efficiency.

Water storage

$$\varepsilon_{H_2O} \leq \xi_{H_2O} \quad 3.37$$

$$\varepsilon_{H_2O} = H_2O_{in} * \eta_{charH_2O} - H_2O_{out} * \eta_{disH_2O} \quad 3.38$$

$\varepsilon_{H_2O}$is the water storage state of charge, ξ_{H_2O} optimal size of water storage, H_2O_{in} is the water input and H_2O_{out} is the water output from the water storage. η_{charH_2O} is the charging efficiency and η_{disH_2O} is the discharging efficiency η_{charH_2O} and η_{disH_2O} is assumed to be 1.

- **Ground water supplier model**

Ground water supplier supplies water to the electrolyzer thanks to a water pumping system requiring electricity. The ground water supplier is comprised of a design parameter giving the size in m^3/h of water. The operational variables are the electricity input (with input connector) for pumping and the water output (with output connector) though they are interlinked, the constraints and the cost expressions (equations 3.6, 3.7 and 3.8.).

- **Ground water supplier model constraints**

$$\mathrm{E_{gw_{in}}} \leq \xi_{\mathrm{gw}} * \chi \quad 3.39$$

$$\mathrm{W_{out}} = \mathrm{E_{gw_{in}}}/\chi \quad 3.40$$

$\mathrm{E_{gw_{in}}}$ is the electricity input for water pumping, χ is the pumping power per m^3 of water at 100m height ($0.36kW/m^3$) [61] and ξ_{gw} is the size (m^3/h) of the water pump.

- **Electricity external grid model**

The electricity external grid allows to injection of electricity into the national grid. It has a grid feed in an operational variable with an input connector and an electricity selling price as a parameter. As the purpose is to produce green hydrogen, the option to buy electricity from the grid is not considered.

- **Hydrogen demand model**

Hydrogen demand is the main load of the energy system. Its model considers it as a parameter with an input connector.

- **Wastewater collector**

The wastewater collector model intends to quantify the available wastewater for other uses after the PV module cooling process. The operational variable within this component is the wastewater output from the PV array with an input connect

3.3.2 Energy System model

The energy system creation consists of using the component models and their connections, additional parameters, variables and states to set it up. For this purpose, four different steps are to follow. After importing from the core of COMANDO the class System and proceeding to the initialization of the component models and creation of the energy system, the component models are then added and connected accordingly through a defined bus. Three typical superstructures are considered in this study to show the interconnections between component models within the energy system models. Hence, the first energy system model superstructure is characterized by an accurate PV component model and RSOECs which stands for both electrolyzer and fuel cell while in the second one, the APV is replaced by the PVC. The third one includes the PVC and whether Alkaline Electrolyzer (AE) or Proton Exchange Membrane Electrolyzer since they have the same component model apart from their input data. **Figure 3, Figure 4**, and **Figure 5** show the details.

The baseline of this study is focused on investigating the optimization results between APV and PVC using.

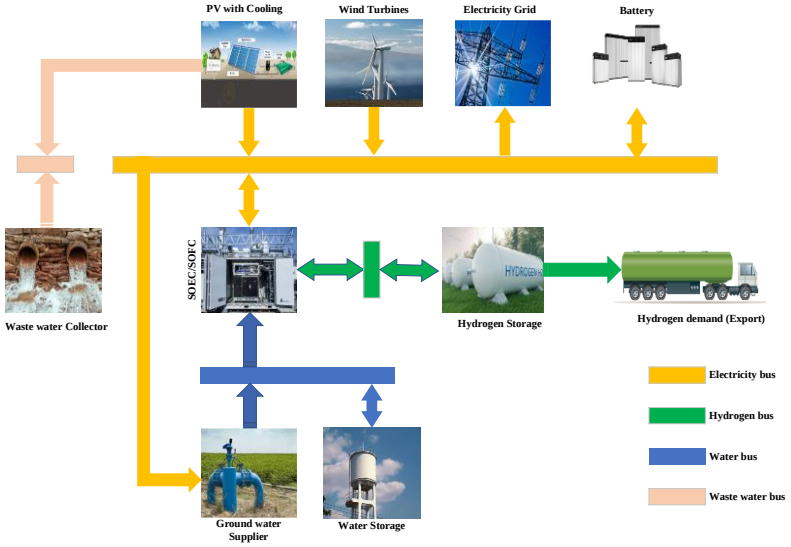

Figure 3: *Energy system superstructure based on PVC and RSOECs*

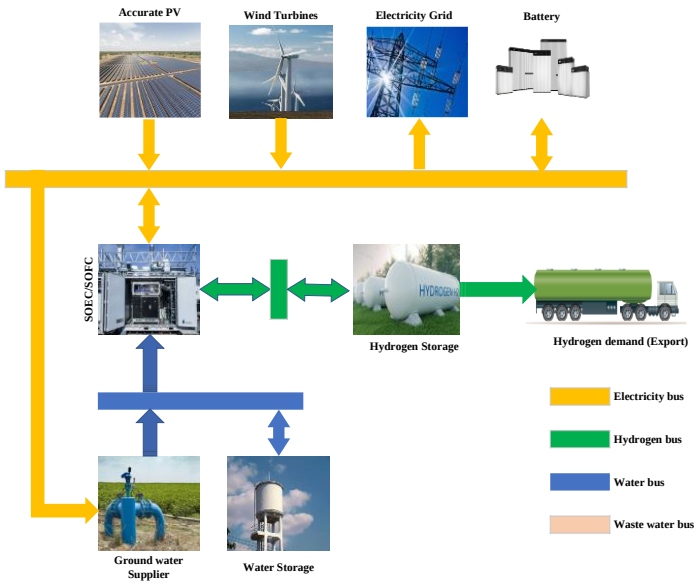

Figure 4: *Energy system superstructure based on APV and RSOECs*

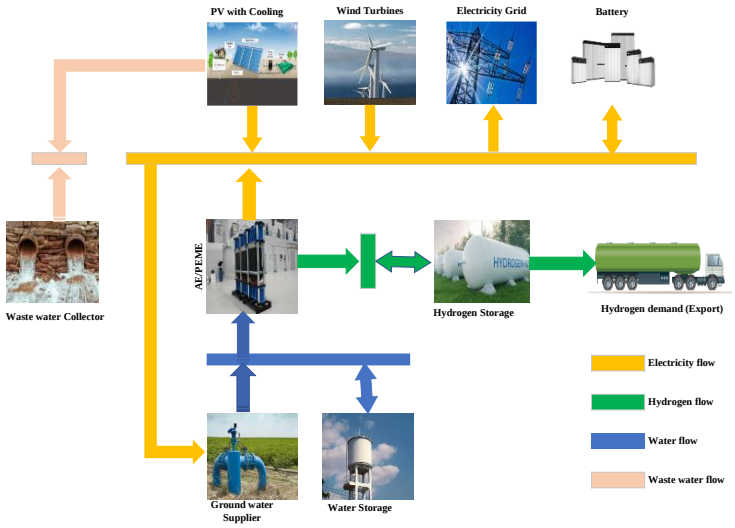

Figure 5: *Energy system superstructure based on PVC and AECs/PEMECs*

3.3.3 Problem formulation

An optimal energy system necessitates optimal decisions at both the design stage and operational stage. Hence, before formulating the optimization problem, the operational scenarios have been considered due to the variability (renewables intermittent and demand variability) coupled with other uncertainties to obtain a reliable design. This leads to a two-stage stochastic programming. We therefore used a cluster data function to determine the scenarios and weights. It allows for the simultaneous consideration of multiple operating scenarios.

3.3.4 Data cluster

Data clustering requires pre-work handling to match the format of the input data with the cluster data configuration. This follows two steps: PV data unstack (as PV is the main energy source with high intermittency) and unstack data normalization. Then, comes the clustering process subdivided into five stages:

- Clustering the normalized data: a number (n) of typical days is set. Those days with the day of maximum and minimum PV output are the only days that can be visualized at the output of the clustering algorithm. By using the Silhouette method, the optimal typical days which correspond to the number having the maximum score have been found for the PV hourly power input data.
- Identification and attribution of PV and demand days per cluster;
- Grouping the days per typical days: Generation of PV scenarios but not yet sorted;
- Sorting the index from smaller to higher and sorting the indices considering arguments;
- Grouping the days per typical days;

3.3.5 Weights

The weights are calculated based on the cluster data; it comprises the frequency of each typical day based on 365 days of the year.

3.3.6 Design and operational problem formulation

- **Objective functions**

The two-stage structure of the problem distinguishes between design and operation-related variables, constraints, and objectives because the design decision and the operational decision are driven by two different vectors.

Our study deals with only design objectives since our energy systems are not buying any commodity (electricity from the grid or hydrogen from another supplier). Therefore, the operational objective of our systems is 0. To define the objective terms, the System class provides the ‘’aggregate_component_expressions’’ method that is used for the cost expressions which have the same identifier for all the component models (“Investment cost” and “Fixed cost”). Hence, it returns the sum of all expressions stored under that identifier in the individual components. The objective function is therefore established including the time steps, the scenarios, and the design objective.

$$C(j) = \mathrm{K} + \mathrm{M} \tag{3.41}$$

$$\begin{cases} \\ \mathrm{T} = min \sum_{j=1}^{k} C(j) \end{cases}^{t_s} \tag{3.42}$$

t_s is the time steps which hour for our case study, K is the capital investment cost while M is the operational and maintenance cost of a given component j, k is a number of components within the energy system and $C(j)$ is the annualized investment cost of a given component j and T is the minimized total annualized investment costs of the overall energy system

- **Problem creation**

COMANDO provides the Problem class, instances of which can be created by the ‘’create_problem’’ method of the System class the optimization problem is based on the energy system set previously, the objective function, the scenarios and the time steps. To make more relevant our optimization problem for the long-term horizon, the seasonal storage constraints of all storage mediums have been included in the problem.

3.3.7 Solution

To solve the optimization problem, the problem structure and input data are translated from the COMANDO representation to a new representation, matching the syntax of the target solver or AML. The solver Gurobi [62] is therefore used to perform the problem-solving and return the solution.

3.4. Sensitivity analysis

3.4.1 Case 1: Influence of electrolyzer technology

The sensitivity analysis aims at examining in this case, the influence of the other technologies of electrolyzer which are mature and commercialized (Alkaline electrolyzer and PEM electrolyzer) on the results of design variables and the total annual investment costs. This will help to find out the best energy system producing green hydrogen with the option to feed electricity into the grid using the PV system that performs with the best baseline optimization results.

3.4.2. Case 2: Hydrogen demand profile impact on the optimization results

This case aims to change the hydrogen demand within the energy system of case 2 while keeping the same daily hydrogen production (15.3 tons). Indeed, the H_2 demand profile that is used so far has an hourly base production of 600 kg (during the night or cloudy times) and an hourly pick production of up to 790.37 kg during the daytime while the second H_2 demand has an hourly base production of 200kg and an hourly pick production up to 2422.6 kg during the daytime.

3.5 Data collection, processing and analysis

The study used historical climate data to validate the optimization models mentioned previously. Hence, the base year of this study is 2019 as it is the most recent data available from the open-data sources used. Hourly data time steps were collected for better resolution.

3.5.1 Meteorological data

Considering the coordinates of the location mentioned in the study area description, open-data sources have been used to get the meteorological parameters input data related to this study. The solar irradiance, ambient temperature, wind speed at 10m of height, and wind power factor were imported from the open-source renewable ninja at the location with the coordinates 7.9628 at the longitude and 16.9522 at the latitude [64, 65].

3.5.2 Economic and technical input data

The economic and technical data are required to validate the model. The discount rate for the case study is assumed to be 5% according to International Monetary Fund (2021) [66]. The replacement cost of the components that their lifetimes do not last for 20 years is included in this study (Stack replacement for electrolyzer and cooling system replacement) as well as other technical parameters are summarized in **Table 1**.

Table 1*: Economical and technical data of each component model*

Component	Specification	Capital Expenditure	Operational Expenditure	Lifetime (Years)	Maximum Capacity	Ref.
PV	Mono-si	205\$/m^2 1,030\$/kWp	10\$/ m^2/year	25	5 km^2 995 MWp	[67,68]
Wind Turbine	Net capacity factor 42.3%	1462\$/kW	43\$/kW/year	25	300 MW	[69]
Water-Cooling System	Steady spray cooling Water storage	12.30\$/m^2 70.2\$/ m^3	-6.4\$/m^2/ year	10 30	PV size	[70,61]
Solid Oxide Electrolyser	Stacks: \$1080	2800\$/kW	2% CAPEX	10.62	100 MW	[71,72,73]
Alkaline Electrolyser	Stacks: 270\$	1512\$/kW	2.5% CAPEX	13.7	100 MW	[74,75]
PEM Electrolyser	Stacks: 400\$	1944\$/kW	2%	10.41	100 MW	[74,75]
Battery		1475\$/kWh	2.5%CAPEX	20	1 GWh	[76]
Hydrogen Storage (160 Bar)	H_2 at 160 bars	350\$/kWh	1% CAPEX	20	8000 kg	[75,77]

Ground Water Supplier	At 100m depth	1663$/m^3/h	2% CAPEX	30	10 /h	[61]
Water Storage	concrete	70.2$/m^3	2% CAPEX	30	50	[61]
Electricity Grid	Electricity selling price		0.14 $/kWh			[78]

3.5.3 Dust and hydrogen demand data

- **Dust accumulation data assessment**

Based on the result of dust accumulation power loss recorded during 21 days (12.46%) in September 2015 [29], hourly dust deposit (0.0247%) has been derived. Afterward, a cleaning per 30 days has been considered for 365 days of the years. As the month of September is part of the months of rainy season, therefore, month with the least dust accumulation within the Sahel, Niger. Hence, the constant monthly dust accumulation depicted by **Figure 6** is the plot of annual dust data based on the scenario of least data accumulation loss throughout the year**.**

- **Hydrogen demand 1 (hourly base demand of 600 kg)**

A ratio x of each hour irradiation over its total daily irradiation has been calculated. This step enables us to generate a same hourly profile of solar irradiation using based on the data frame of the ratio x. Then, this ratio x generated is input in the equation 3.43 to generate the hydrogen demand profile (λ_1) of 15.3 tons H_2 demand per day as depicted the **Figure 12**.

$$\lambda_1 = 600x + 600 \qquad 3.43$$

- **Hydrogen demand 2 (hourly base demand of 200 kg)**

Similarly, the same daily hydrogen quantity of 15.3 tons per day is consider generating the second hydrogen (λ_2) using the same ratio x that is input in the equation *3.44*. **Figure 13** presents its profile.

$$\lambda_2 = 7005x + 200 \qquad 3.44$$

3.5. Models' assumption

- Constant hourly power loss due to the dust accumulation generated from 21 power loss in Niamey was applied to Agadez, the location of study even if it is a dustier city than Niamey.
- The water temperature to cool down the PV module is 32°C [79]
- Inflation has not been considered for the input costs data and costs in Euro currency are converted into dollar US June 2023 (1 EURO =$ 1.08) based on the actual cost found from data sources.
- One time cleaning cost in Italy is 2500 €/MW (2.5 €/kW) [68] corresponds to one month cleaning cost is considered for 12 months of the years.

Chapter 3

4. Results and Discussion

4.1. Data generated results

Several input data have been processed to perform the optimization model validation. The dust data which is input data for the accurate PV was processed based on an experimental result done in Niamey by Dajuma *et al* [29] since no dust study has been performed in Agadez, then following the accurate PV power output per m^2 and the PV power with cooling output that are the main input data of the optimization problems. The cooling system's working power and finally, two hydrogen demands were simulated to provide hydrogen input data to the problems and pump power consumption respectively.

4.1.1. Dust data

The result shows an increase in dust loss from 0.02% on the first hour after cleaning to 17.80% on the thirtieth day.

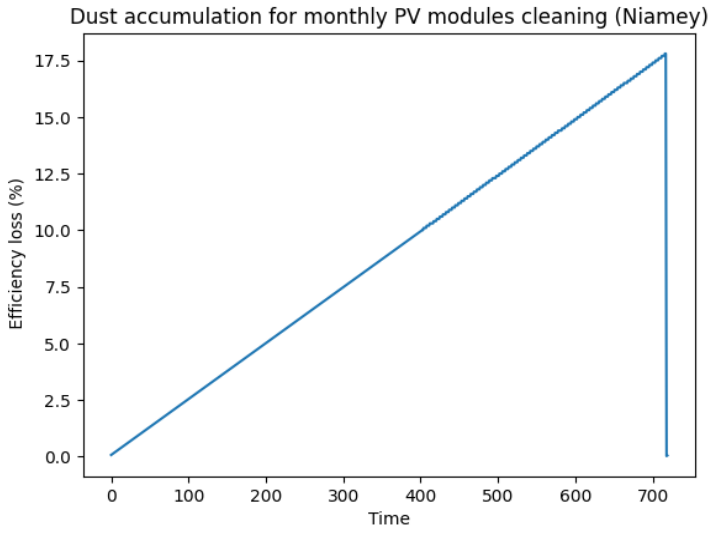

Figure 6: *Dust accumulation based on monthly PV modules cleaning*

4.1.2. Cells' temperature

The cell overheating observed in **Figure 7** goes up to 74.06° whereas the PV module gives the best performance at 25°. Combined with the dust loss decreases the maximum power output per square meter up to 0.177 kW (**Figure 9**) instead of 0.199 kW at the STC conditions while **Figure 10** of the PVC shows a maximum power per square meter of 0.187 kW so 10 W of power gap.

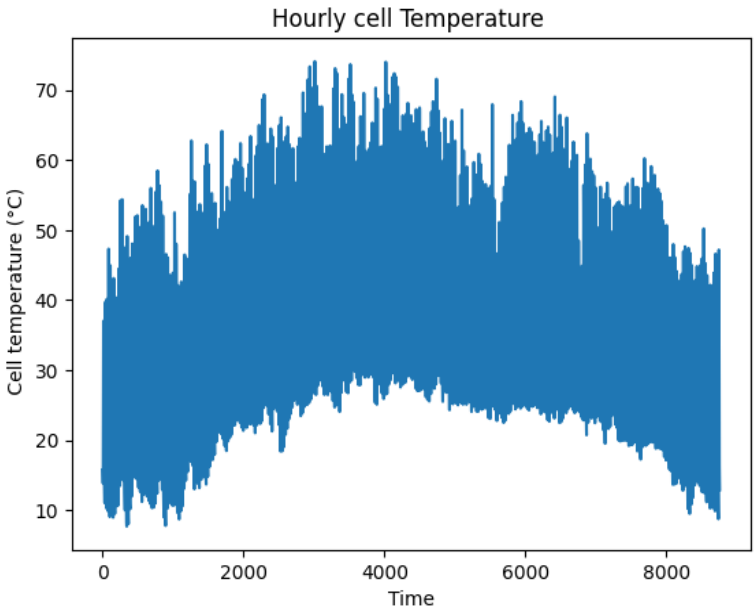

Figure 7*: Module cells' temperature cell*

4.1.3. Accurate PV array power per m² process

Solar irradiance, wind speed at 10m, ambient temperature and dust accumulation data are input into the equations 3.1, 3.2, 3.3, 3.3 and 3.4 to get the power output of the APV. **Figure 7** and **Figure 9** show respectively the results of the cell temperature and the power output of the APV.

4.1.4. PV with cooling power per m² process

The cooling PV power output has been obtained following the equations 3.9, 3.10, 3.11, 3.12, 3.13 and 3.14 thanks to the irradiance, the ambient temperature, and wind speed at 10m, the pump power consumption data**. Figure 10** presents the power output of the PVC.

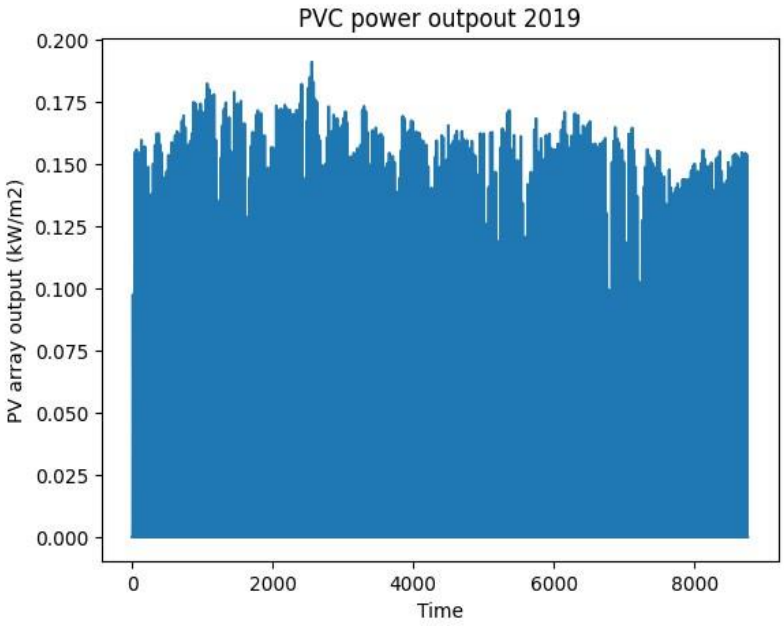

Figure 9: *Accurate PV power output*

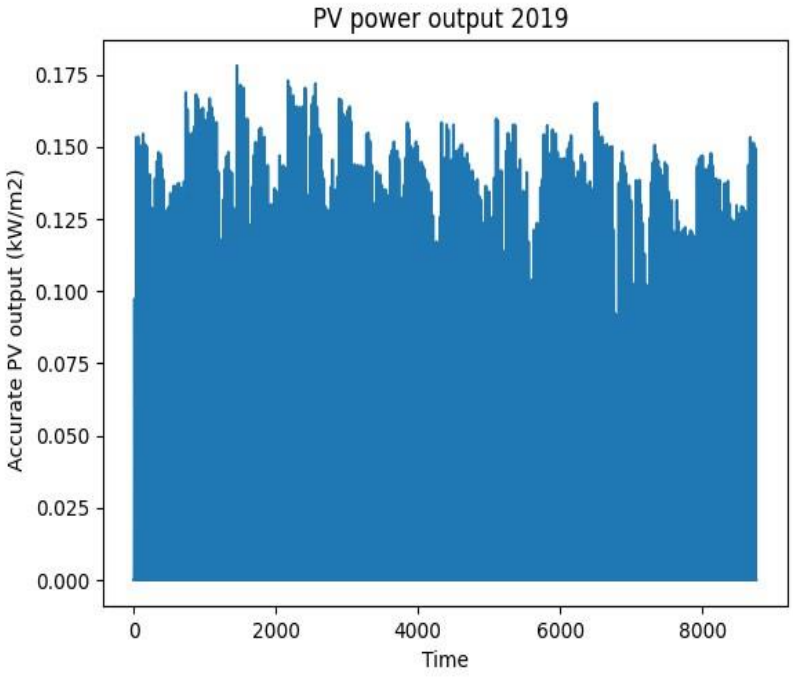

Figure 10: *PV with cooling power output*

- **Cooling optimal activation**

The result of equation 3.13 gives an amount of 3.4W power requirement for pumping water at 100 m height to cool down 1 m^2 of PV modules. The power optimization of the PVC is done based on this data. **Figure 11** shows the water-cooling activation profile for 24 hours.

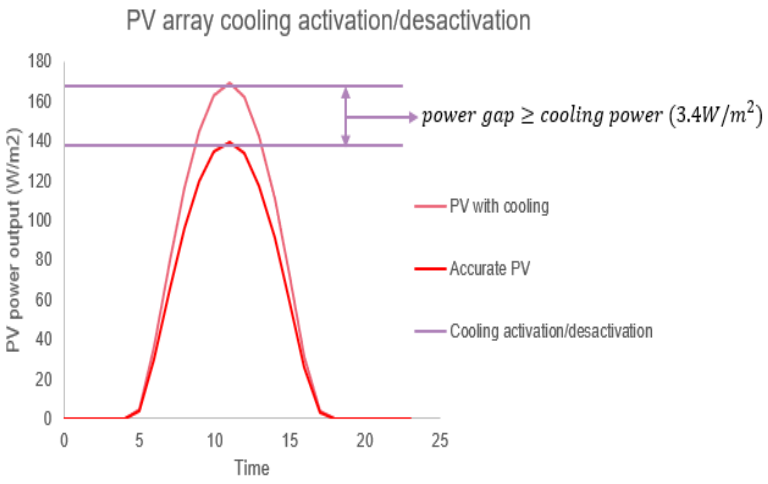

Figure 11: *Cooling activation condition*

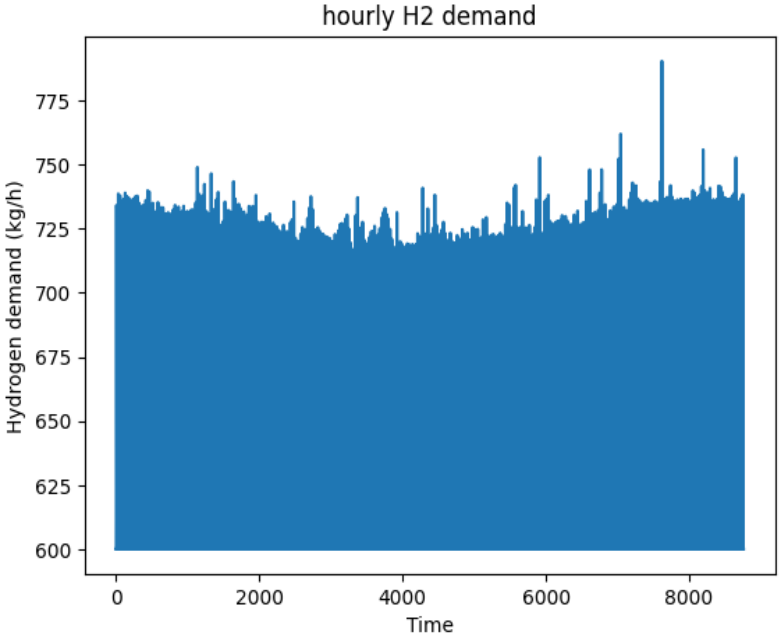

Figure 12: *Hydrogen demand 1 for baseline case*

4.1.5. Hydrogen demands

As shows the **Figure 12** the minimum hydrogen production is 600 kg during the night or no cloudy day and the pick production occurs during the day driven by the PV while the second demand depicted by **Figure 13** shows a base production of 200 kg with pick production during the daytime.

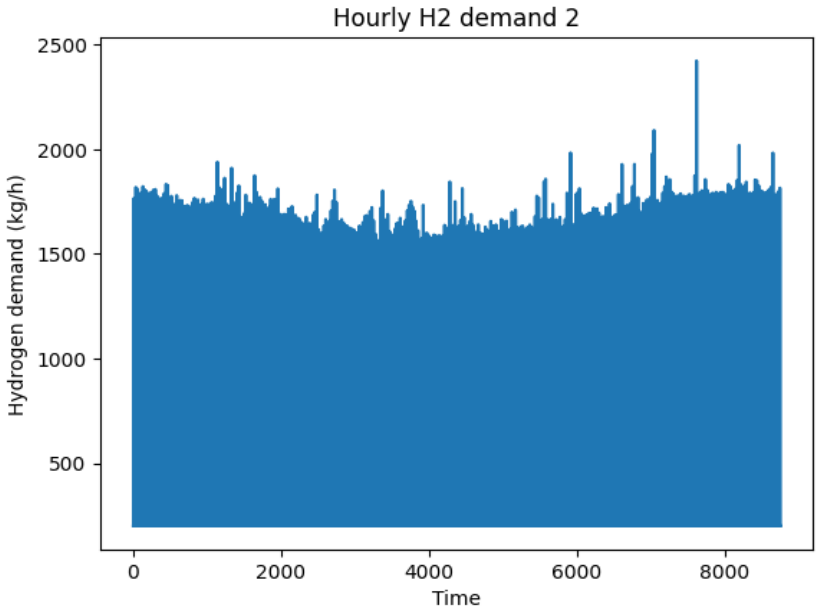

Figure 13*: Hydrogen demand 2*

4.1.6. Data cluster results

Silhouette method was used to determine the optimal cluster number. It was found on two typical days. **Figure 14** shows the result for the case of accurate PV power output per square meter. Four different typical days will be visualized at the output of the algorithm since the maximum and the minimum are added to the two typical days found, therefore, the optimization is based on these two different scenarios in addition to the two particular days as shown in **Table *2***.

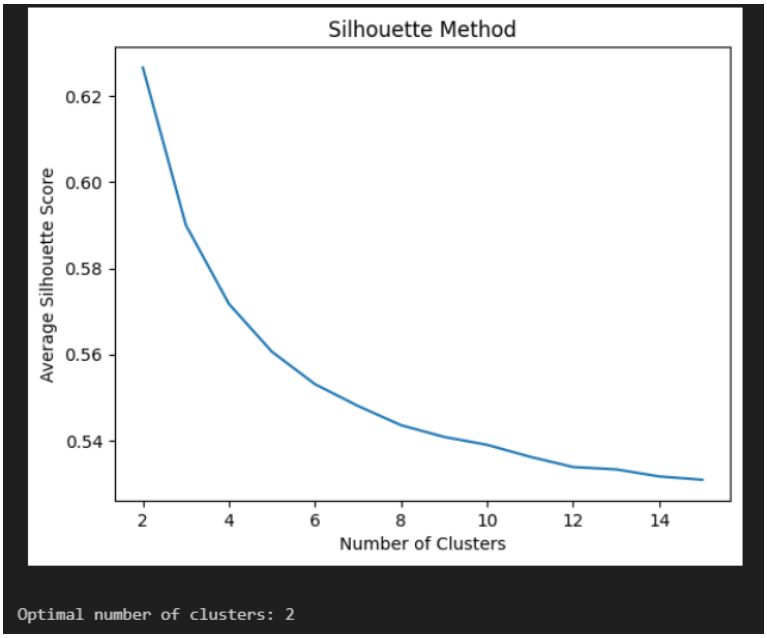

Figure 14: *Optimal cluster number using Silhouette method*

Table 2: *PV scenarios and weights*

Accurate PV		PV with cooling	
Day (Scenario)	Weight	Day (Scenario)	Weight
60	1	106	1
232	1	118	175
255	178	232	1
291	185	318	188
Total	365	**Total**	365

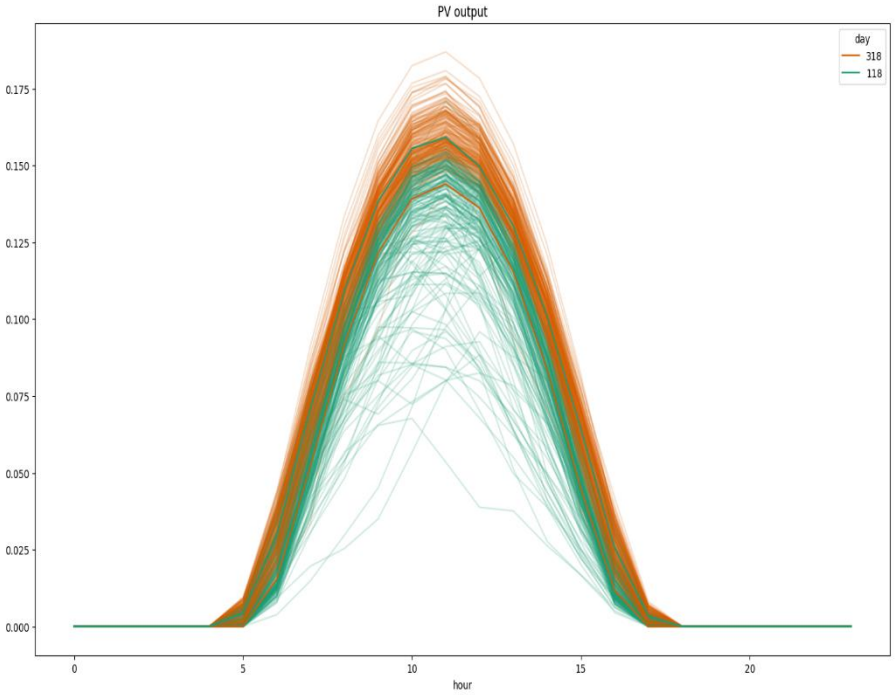

Figure 15*: PV with cooling clustered data plot*

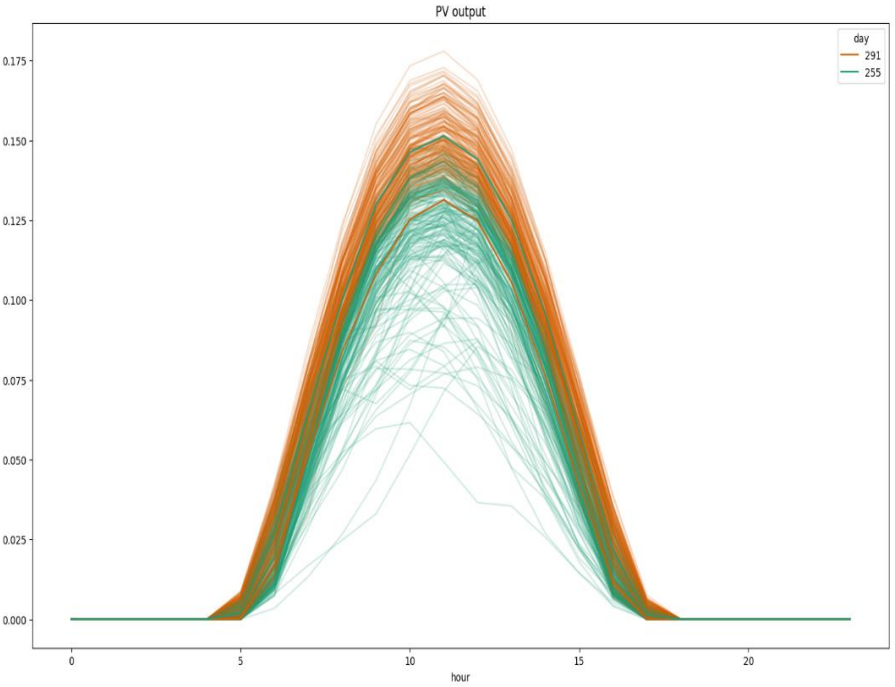

Figure 16*: Accurate PV clustered data plot*

Figure 16 and **Figure 15** show the PV power output per square meter cluster data for respectively the APV and PVC. They are all characterized by two scenarios corresponding to two typical days. The scenario corresponding to day 255 with a frequency of 178 days represents the worse scenario in terms of power output while day 291 with a frequency of 185 days represents the best scenario for the APV. Regarding the PVC, the worst scenario matches with day 118 while the best scenario corresponds to day 318 with a frequency of 188 days. For both APV and PVC, the best scenarios have higher weights.

4.2. Baseline optimization results

As mentioned earlier, this section intends to show the results of the accurate PV and the PV with cooling. The optimization results provide the actual values for the decision variables (Design and Operation) therefore, the optimal design, the total annualized costs and the operating results as well are visualized.

Table 3*: APV and RSOECs optimization Results*

System component	**Optimal size**	**Capital expenditure ($ million)**	**Operation expenditure ($ million)**
Accurate PV	1.38 km^2 274.22 MWp	20.04038	13.77795
RSOEC	74.71 MW	22.46370	2.09197
Wind power	38.76 MW	28.33660	1.66679
H2 storage	6,241 kg	0.17528	0.02184
Ground Water supplier	8.05 m^3/h	0.00087	0.00027
Water storage	84.93 m^3	0.00039	0.00012
Battery	0 kWh	0.00000	0.00000
Grid fed in (GWh)	401.171		
Electricity sold to the grid	$56.164 million		
Actual H_2 investment cost	$32.42 million		
Total annualized costs	**$88.58 million**		

Table 4: *PVC and RSOECs Optimization results*

System component	Optimal size	Capital expenditure ($ million)	Operation expenditure ($ million)
PV with cooling	1.305 km^2 259.78 MWp	24.81667	4.69955
RSOEC	71.93 MW	21.62701	2.01406
Wind power	39.76 MW	29.06571	1.70967
H2 storage	6,122 kg	0.17196	0.02184
Ground Water supplier	8.05 m^3/h	0.00087	0.00027
Water storage	83.43 m^3	0.00038	0.00012
Battery	0 kWh	0.00000	0.00000
Grid fed in (GWh)	372.323		
Electricity sold to the grid	$52.13 million		
Actual H_2 investment cost	$32 million		
Total annualized costs	**$84.13 million**		

The figures below show the optimal operating results of the energy of both energy systems.

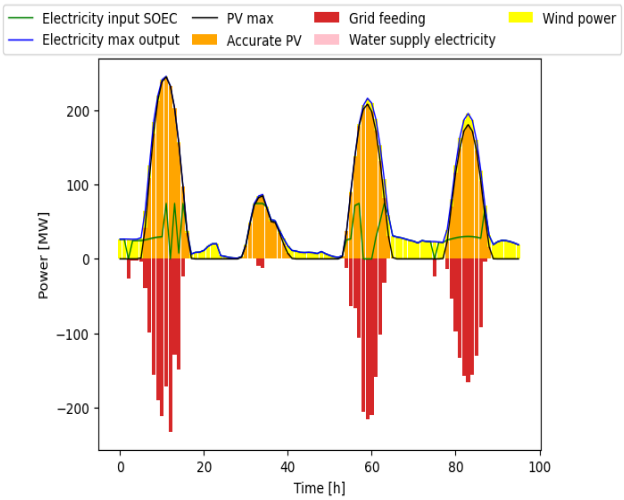

Figure 17: *PVC system electricity bus variables*

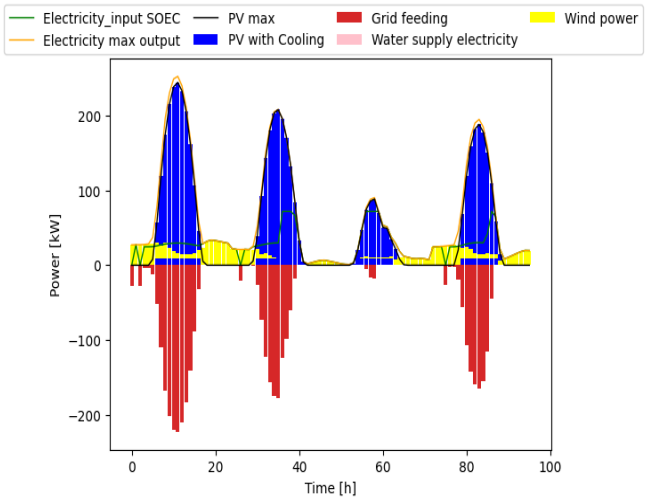

Figure 18: *Accurate PV system electricity bus variables*

Optimization results of the two different energy systems namely Accurate PV in **Table 3** and PV with cooling in

System component	**Optimal size**	**Capital expenditure ($ million)**	**Operation expenditure ($ million)**
Accurate PV	1.38 $km2$ 274.22 MWp	20.04038	13.77795
RSOEC	74.71 MW	22.46370	2.09197
Wind power	38.76 MW	28.33660	1.66679
H2 storage	6,241 kg	0.17528	0.02184
Ground Water supplier	8.05 $m3$/h	0.00087	0.00027
Water storage	84.93 $m3$	0.00039	0.00012
Battery	0 kWh	0.00000	0.00000
Grid fed in (GWh)	401.171		
Electricity sold to the grid	$56.164 million		
Actual H2 investment cost	$32.42 million		
Total annualized costs	**$88.58 million**		

Table *4* show various results for system design and operation under the same conditions, solid oxide electrolysis for green hydrogen production with hybrid solar and wind as electricity generators with option to sell the surplus of electricity to the grid. For the system of Accurate PV, sizes of 274.22 MWp and 38.76 MW are required respectively for the PV size and wind farm size to meet 15.3 tons and 55.845 tons respectively for daily and yearly hydrogen production while feeding an amount of 401.171 GWh into the grid whereas sizes of 259.78 MWp and 39.76 MW is required respectively for the PV size and wind farm size to meet the same

hydrogen demand while feeding an amount of 372.323 GWh into the grid.

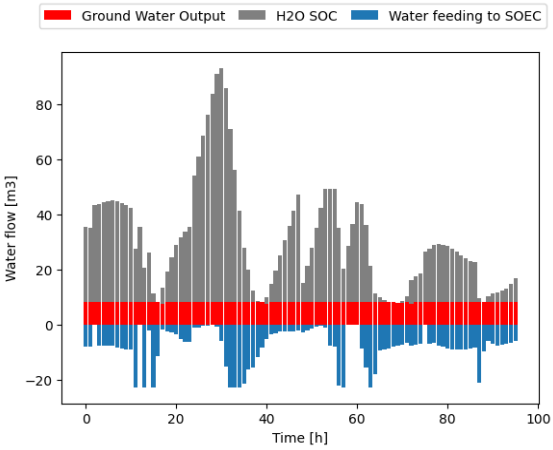

Figure 22: *Accurate PV water bus variables*

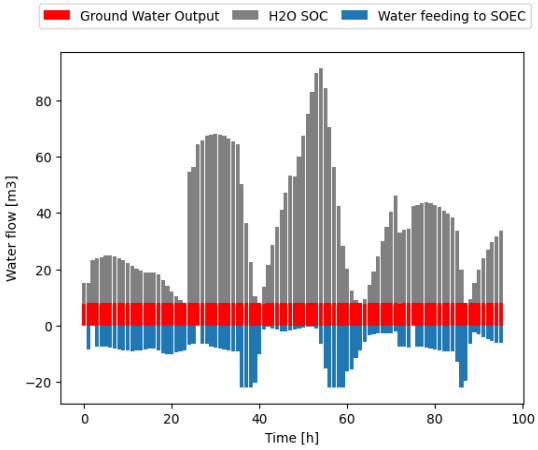

Figure 21: *PVC water bus variables*

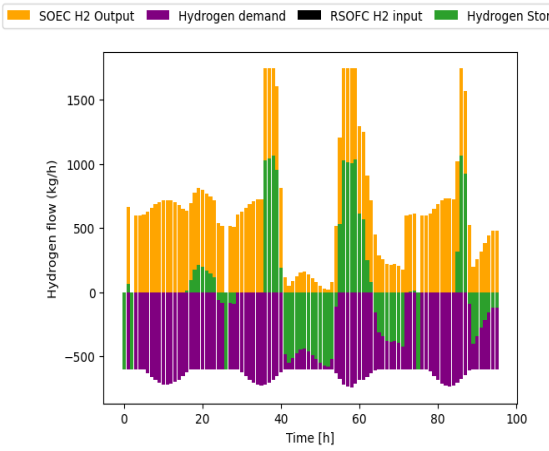

Figure 20: *PVC system hydrogen bus*

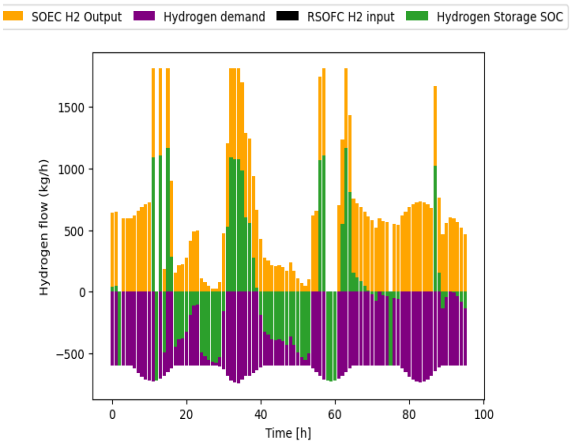

Figure 19: *Accurate PV system hydrogen bus*

It can be drawn that improving the efficiency of the PV modules through cooling by minimizing cell overheating and dust accumulation leads to minimizing (14.14 MWp reduction) the PV size while increasing the power production even if a slight increase in the size of wind size has been noticed (1 MW). This means that the installation of 13.13 MWp and 0.075 km^2 (7.5 hectare) PV plant has been saved. Therefore, the electricity excess fed to the grid is decreased from 401.171 to 372.323 GWh. This optimization results look better since the main purpose is to meet the hydrogen demand. **Figure 17**: PVC system electricity bus variables and **Figure 18**: Accurate PV system electricity bus variables depict the operating results of the electricity flow for the two energy systems based on the 4 typical days. For both, the electricity fed into the grid is mainly driven by the PV output for three typical days and slight feeding during the day of minimum PV electricity production, this is due to the large size of the PV concerning the wind turbines size as well as the intermittent production of

the PV. Moreover, wind electricity production is weak during the day and significant during the night giving a better option than battery storage.

Figure 21 and **Figure 22** show that the output of the electrolyzer is a bit discontinued for APV than the PVC this is due to the slight oversize of the electrolyzer for the APV system over the PVC system, while shutting down all the electricity is fed into the grid, one of the reasons why the electricity fed is greater for the APV system. Moreover, the RSOECs did not perform at all as fuel cells since the hydrogen input to the RSOECs is 0. This can be explained by the fact that it is not effective to use the hydrogen produced for electricity purposes while having two electricity sources and no electricity demand as a priority.

Figure 19 and **Figure 20** show that water is pumped full-time for both of the systems and the water supply to the electrolyzer follows its hydrogen output profile since electricity and water are the main feedstock for hydrogen production.

Economically, the results show that the PV installation cost increases from $20.040 to $24.82 million due to the additive cost for PV cooling system installation cost while the maintenance and operational cost decreases from $13.78 million to $4.70 million with a total annualized cost of $84.13 million against $88.58 million. Thus, $4.45 million is the saved cost but if the electricity sold amount is withdrawn from the total annualized costs, a slight difference of $0.42 million has been noticed for the actual cost of green hydrogen production considering the surplus electricity selling options. As the analysis is performed for the same lifetimes for both PV systems, the next analysis will examine how extending the lifetime of the PV by applying water cooling and the electrolyzer technologies and cost can affect the optimized sizes and the costs.

4.3. Water-cooling system performance

The water-cooling system integrated with the module operates as explained in section □**,** The first condition is based on the saving energy gap, if this condition is satisfied and the cell temperature assimilates to the module's temperature reaches the MAT, the cooling system can perform the cooling of the PV array. For the worse scenario characterized by the typical day 118 for the PVC, it is noticed that, at 7 am, the module temperature is at 40.93°C while the pumping activation in **Table 5** is not allowable (cooling activation OFF=0) meaning that the power possible to save is less than 0 if the cooling operates. Then, at 8 a.m. this temperature increases up to 50.48 °C while the cooling activation is allowable (ON=10). Therefore, the first cooling was performed dropping the module temperature from 50.48 °C to 42.2°C. Since this value is beyond the MAT, the cooling

continues from 9 to 10 a.m. with a temperature drop up to 37.63 °C and stop but the heating rate raises the module temperature to 41.67°C at 11 a.m., therefore, the third cooling was performed from 11 to 12 p.m. cooling down the module at 37.34°C. A last cooling was done from 3 p.m. to 4 p.m. dropping the temperature from 44.5°C to 35.5 to maintain the module operating temperature below the MAT.

Finally, 4 cooling cycles are required to keep the PV modules working optimally at 8-9 a.m., 9-10 a.m., 11 a.m.-12 p.m. and 3-4 p.m. respectively with cooling rates calculated according to 3.18 of 8.3°C /h, 4.6°C/h, 4.3°C/h and 5.1°C/h while the heating rates calculated based on equation 3.15 are respectively 7.5°C/h, 5.6°C/h, 1.94°C/h and -8.52°C/h. **Table 5** highlights the overall results.

Table 5*: Water-cooling system performance results*

Hour	*Module temperature without cooling*	*Cooling activation*	*The heat removed by cooling*	*Heating rate*	*Module temperature with cooling*
0	25.99	0	0.00	-0.64	25.99
1	25.35	0	0.00	-0.54	25.35
2	24.81	0	0.00	-0.46	24.81
3	24.36	0	0.00	-0.45	24.36
4	23.90	0	0.00	1.11	23.90
5	25.02	0	0.00	7.19	25.02
6	32.21	0	0.00	8.72	32.21
7	40.93	0	0.00	9.56	40.93
8	50.48	10	8.28	7.51	42.20
9	57.99	10	4.57	5.62	37.63
10	63.61	10	0.00	4.04	41.67
11	67.65	10	4.33	1.94	37.34
12	69.59	10	0.00	-2.65	33.01
13	66.93	10	0.00	-6.09	26.92
14	60.84	10	0.00	-7.97	34.89
15	52.88	10	5.11	-8.53	43.42
16	44.35	0	0.00	-8.33	38.31

17	36.02	0	0.00	-3.04	36.02
18	32.98	0	0.00	-1.31	32.98
19	31.68	0	0.00	-1.27	31.68
20	30.41	0	0.00	-1.18	30.41
21	29.23	0	0.00	-1.06	29.23
22	28.17	0	0.00	-0.98	28.17
23	27.19	0	0.00	-1.20	27.19

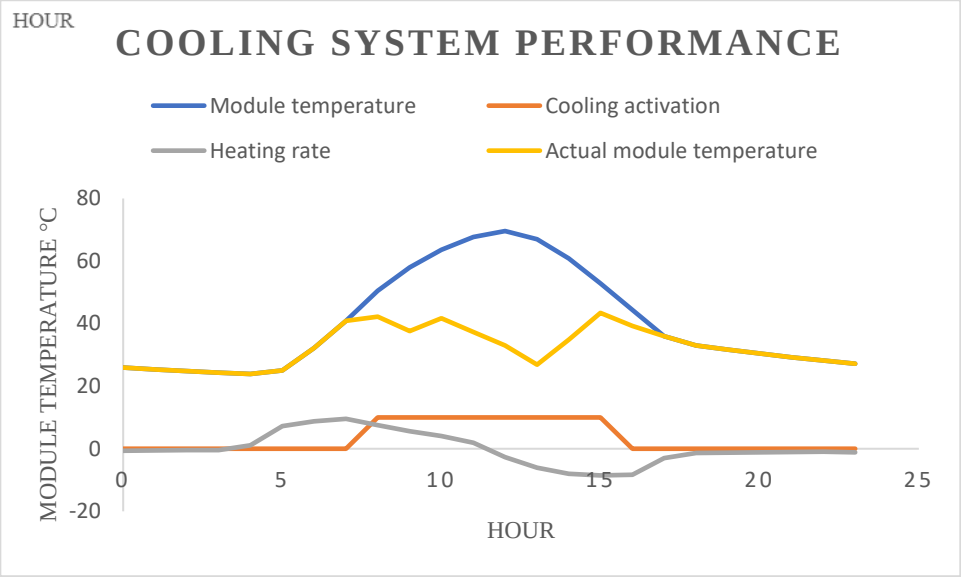

Figure 23: *Module temperature, heating rate, cooling module temperature and cooling activation results*

4.4. Sensitivity analysis results

4.4.1. Results of case 1

The energy system of the PVC performing with the most mature electrolyzer (alkaline electrolyzer) shows a result of an increase of the PVC, wind turbines, alkaline electrolyzer and even the hydrogen storage compared to the baseline case. This increase in size is more significant with the system of using the PEMECs. Comparing **Table 6** and **Table 7**, the total annualized cost of the AECs is less than PEMEs with a difference of $14.62 million. The design results confirmed this difference in cost investment because the sizes of PVC, wind turbines, PEMECs the mains and costly components of the PEMECs' system require additional sizes respectively of 33.98 MWp, 5.37MW, 1.42 MW for the alkaline system. This oversize led to a significant amount of the electrical grid

feeding for the PEMECs' system (76.66 MWh). Though this energy is sold to the grid the alkaline system performs with a minimized actual hydrogen investment cost which is the cost left from the total annualized cost if the electricity selling revenue is considered. Two factors explain why alkaline gives the best results in this study, PEMEC CAPEX (1944$/kW against 1512$/kW) is greater than the alkaline one while alkaline efficiency is greater than the PEMECs one (68.1% against 61.1%). Hence, an alkaline electrolyzer of an option for green hydrogen production even though this technology has the drawback of limited current density and low hydrogen outlet pressure and low H_2 gas purity.

Table 6: *Alkaline electrolyzer and PVC results*

System component	**Optimal size**	**Capital expenditure ($ million)**	**Operation expenditure ($ million)**
PV with cooling	1.45 km^2 289.85 MWp	27.55	5.22
AECs	97.74 MW	10.02	3.69
Wind power	47.32 MW	34.59	2.03
H_2 storage	6,173.7 kg	0.173	0.02
Ground Water supplier	8.05 m^3/h	0.00087	0.00027
Water storage	84.08 m^3	0.00038	0.00012
Battery	0 kWh	0.00000	0.00000
Grid fed in (GWh)	403.40		
Electricity sold to the grid	$56.48 million		
Actual H_2 investment cost	26.84$ million		
Total annualized costs	**$83.33 million**		

Table 7*: Optimization results of PVC and PEM electrolyzer*

System component	**Optimal size**	**Capital expenditure ($ million)**	**Operation expenditure**

			($ million)
PV with cooling	1.68 km^2 335.98 MWp	31.96	6.05
PEMECs	99.16 MW	15.10	3.85
Wind power	52.69 MW	38.52	2.26
H_2 storage	6,143.6 kg	0.173	0.02
Ground Water supplier	8.05 m^3/h	0.00087	0.00027
Water storage	83.7 m^3	0.00038	0.00012
Battery	0 kWh	0.00000	0.00000
Grid fed in (GWh)	480.06		
Electricity sold to the grid	$67.20 million		
Actual H_2 investment cost	$30.73 million		
Total annualized costs	**$97.95 million**		

4.4.2. Results of case 2

The load profile is a key factor inflicting the optimization results. Since hydrogen is the only demand of the system, this study aims to look at the impact of the hydrogen profile on the design and optimized cost of 15.3 tons daily hydrogen production with the system of PVC (25 years lifetimes) and the alkaline electrolyzer. Using the second hydrogen demand which requires 200 kg per hour at sunset and maximizes the production during the daytime to meet the 15.3 tons per day the total annualized costs drop from $83.33 million (**Table 6**) to $ 65.68 million (**Table 8**) meaning $17.65 million of saving. The design variables' results show a significant increase in PVC size 348.22 MWp against 289.85 MWp mainly 58.37 MWp difference while the wind turbine size drops from 47.32 MW to 15.78 MW meaning 31.54 MW left. Moreover, the hydrogen storage drops as well from 6,173.2 kg to 1,985 kg whereas the electrolyzer reaches its maximum of 100 MW against 97.73 MW. It can be drawn that the hydrogen demand profile is a key factor in giving the best optimal design and total investment cost for a hydrogen production project if it is based on hybrid solar and wind energy. The profile should follow the renewable having the best potential. Wind turbines are more expensive than PV. However, adding wind to PV is more cost-effective than using a battery according to these results. Electricity storage option is still expensive and hybrid

systems are cost cost-effective than solar with electricity storage. Improving the PV performance through water-cooling renders PV technology more effective within the Sahel.

Table 8: *Optimization results PVC, AECs and hydrogen demand 2 energy system*

System component	Optimal size	Capital expenditure ($ million)	Operation expenditure ($ million)
PV with cooling	1.74 km^2 348.22 MWp	33.11	6.27
AECs	100 MW	10.25	3.78
Wind power	15.78 MW	11.54	0.68
H2 storage	1,985 kg	0.056	0.0069
Ground Water supplier	8.27 m^3/h	0.0009	0.00028
Water storage	98.51 m^3	0.00045	0.00014
Battery	0 kWh	0.00000	0.00000
Grid fed in (GWh)	431.81		
Electricity sold to the grid	$60.45 million		
Actual H_2 investment cost	$3.22 million		
Total annualized costs	**$65.68 million**		

4.5. Water requirement for cooling PV for the energy system of case 3

The PVC cooling requires water to cool to keep the module at the MAT considering the best optimization results which are the results of section **4.3**. Hence, the study intends to determine the number of cooling cycles of PV array cooling required per typical day and the water consumption needed to meet this goal **Figure 24**, **Figure 26** and **Figure 25** show the profile of module during the each typical day and it can be noticed that the cooling enables to maintenance of the module temperature around the MAT (40°C). **Table 9** summarizes the number of cooling cycles and the water consumption. The results show that the typical day 232 does not require any cooling whereas day 106 requires the same number of cooling cycles (4) as the day 118 while day 316 performs with 3 cooling cycles. The amount of water needed for 1.74 km^2 of PV array size (348.13 MWp)

is 12,258 m^3 per cooling cycle and an amount of 49,032 m^3 is required for both days 106 and 118 whereas 36.774 m^3 is required for day 318.

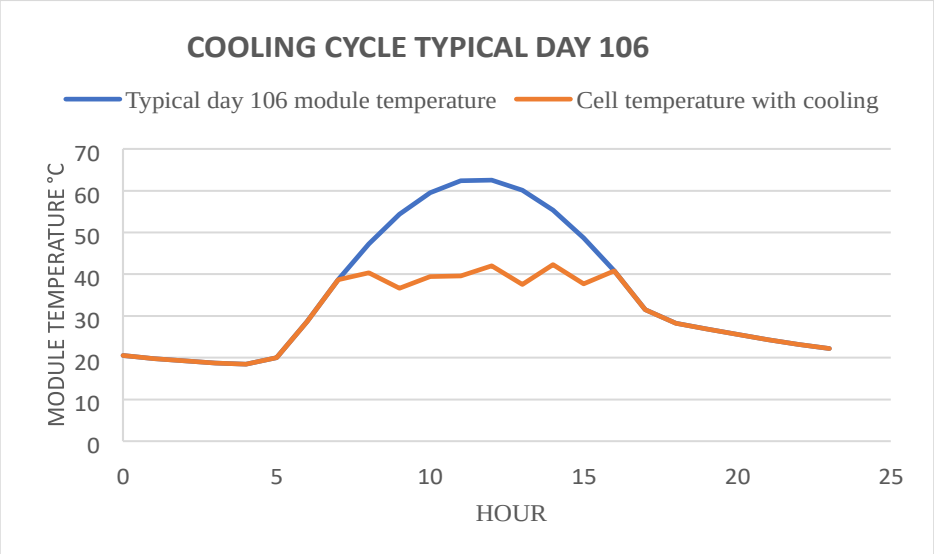

Figure 24: *cooling profile for typical day 106*

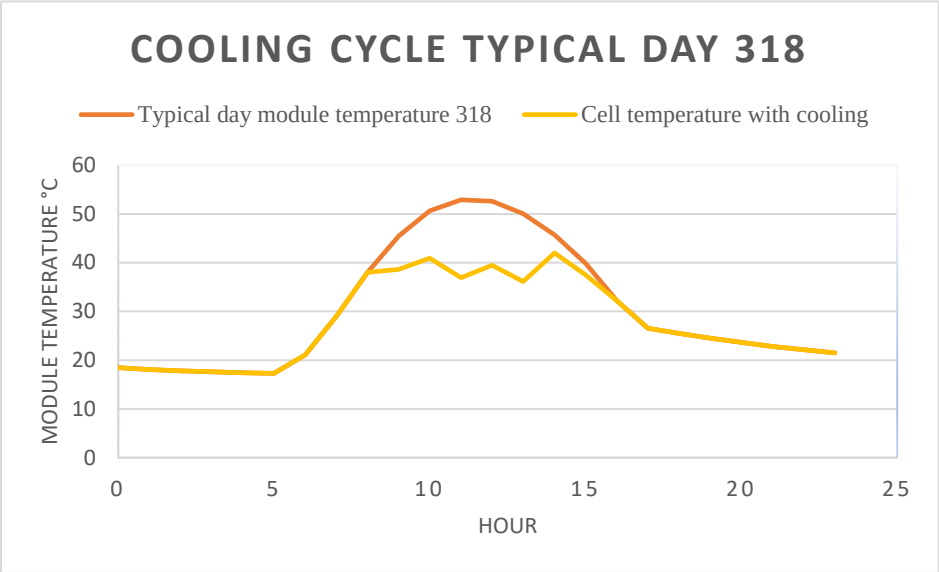

Figure 26: *Cooling profile for typical day 318*

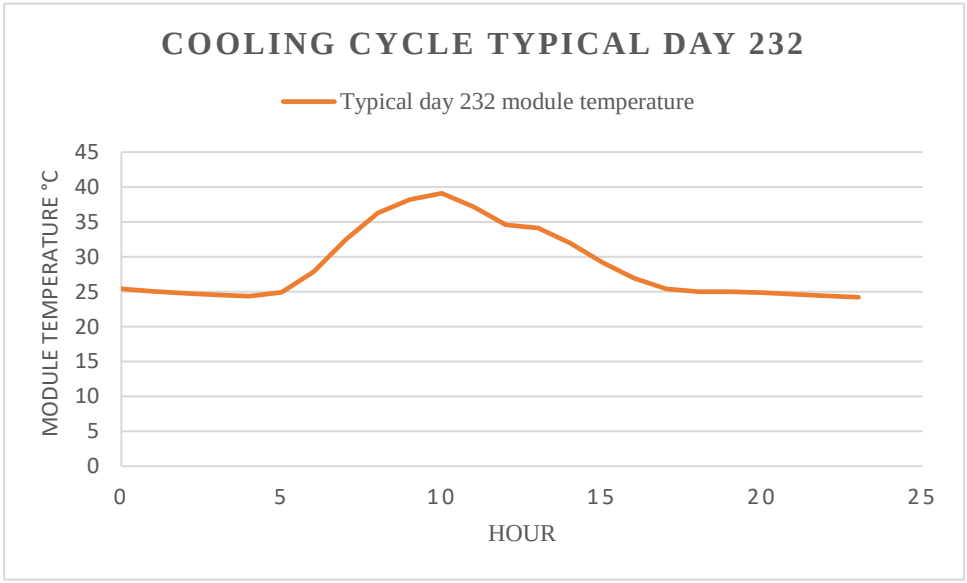

Figure 25: *Module temperature profile of typical day 232*

***Table 9**: Cooling cycle and water requirement per typical day*

Typical day	*106*	*118*	*232*	*318*
Number of the cooling cycle	4	4	0	*3*
Water requirement per cycle	*12,258 m^3*			
Water requirement per typical day	49,032 m^3	49,032 m^3	0 m^3	36.774 m^3

5. Conclusion and recommendation

This study was carried out with the help of the COMANDO energy system model framework, to identify the optimal type of PV to utilize for cost-effective green hydrogen production. Two PV models were examined, an accurate PV including the module's temperature, wind and dust accumulation on the PV array to give a PV power output close to the PV array output in severe environment. The second model integrated a water-cooling system into a PV array with the optimization of the power requirement for cooling to improve the performance of the accurate PV array. Both APV and PVC were used for the optimization of green hydrogen production under several energy system models. This optimization aims at meeting a daily hydrogen production of 15.3 tons per day and about 5,600 tons per year. RSOECs were the baseline of this study. To supply this hydrogen demand, the system configuration of APV and RSOECs, the sizes of 274.22 MWp, 38.76 MW and 74.71 MW for APV, Wind turbines, and RSOECs were respectively found. For the system of PVC, better results are found. The PV size decreases from 274.22 MWp to 259.78 saving a PV module installation of 13.13 MWp and 7.5 hectares of land requirement. However, the wind turbine size increases by one unit from 38.78 to 39.76 MW while the electrolyzer size decreases from 74.71 to 71.93 MW. These results are due to the operating efficiency of the PV improved thanks to the water-cooling system which limits the PV cell overheating to the MAT (40°C) and the dust accumulation loss as well. Therefore, this affects directly both the design and investment cost decisions. Economically, the total annualized investment cost drops from $88.58 million to $84.13 million for the PVC. However, it has been found that the oversize of the APV leads to a high production electricity surplus that is sold to the grid (401.17GWh for APV and 372.32 GWh for PVC), and if the electricity sold revenue is considered for 0.14$/kWh, the difference becomes tight ($0.42 million).

Further analysis of systems configuration using AECs and PEMECs with the PVC to investigate how the electrolyzer technologies can influence the optimization results showed that AECs performed with better results than the PEMECs and the RSOECs with a total annualized investment cost of $83.33 million while PEMECs and RSOECs give respectively $97.95 million and $84.13 million. It can be drawn that the cost of an electrolyzer is a key factor while performing an optimization problem because PEMECs are expensive. Nevertheless, RSOECs which are the most expensive electrolyzers and are still in the development process total annualized investment cost competes with the AECs' cost because of the high efficiency of this technology. Therefore,

improving the electrolyzer's efficiency and reducing its cost will definitively promise better optimization results.

Finally, the hydrogen demand was changed in the alkaline based system, this hydrogen demand shows a profile of high peak production during the daytime (up to 2422.6 kg) a low hourly production (200kg as hourly minimum production). The results show a significant impact on both the optimal design and costs. The cost drops from $83.33 million to $65.68 million led by a significant increase in the PV size from 289.85 MWp to 348.22 MWp and the wind turbine size drop 39.76 MW to 11.54 MW. For Hydrogen production in the Sahel with hybrid solar and wind, it will be profitable to produce more hydrogen with solar and use wind for the minimum production since the results of all the configurations did not choose the battery storage option.

The added value of the PVC energy system is the wastewater that can be reused in the agriculture sector which is facing surface water scarcity for food production in drought season without investing in solar water pumping system. Hence, this study is a typical energy system making the nexus energy-water-food security as large-scale PVC will supply more water to improve food security in Niger and Africa in general.

During this work, there were topics found unanswered or left for future work. Future work can focus on the following recommendations:

- A study on dust loss assessment throughout the year and the impact of dust accumulation et cells overheating on the PV module could improve the results of the APV versus PVC.
- Perform a qualitative and quantitative analysis on the impact of the wastewater collected after PV array cooling on agricultural production to enhance food security in the Sahel;
- Perform a study on the impact of water requirement for cooling on the groundwater reservoir and sensitivity analysis on the cooling system to optimize water consumption for PV array cooling in the study area;
- Perform a literature review on Green Hydrogen production system components costs to highlight the accurate cost of components to perform an accurate economic analysis because there is too much inconsistency in the cost of components in the literature.

6. References

1. Renewable Energy Agency I. World energy transitions outlook 2022 executive summary. 2022.

2. World Resources Institute. Climate Watch Historical GHG Emissions. Washington DC 2021. https://www.climatewatchdata.org/ghg-emissions.

3. Deloitte. Green hydrogen: Energizing the path to net zero. 2023.

4. Robert Perkins. cop 26 discussion about conversional sources of energy1. 2021;

5. Renewable Energy Agency I. Global hydrogen trade to meet the 1.5°c climate goal part i trade outlook for 2050 and way forward. 2022.

6. International Renewable Energy Agency. Geopolitics of the energy transformation: the hydrogen factor. 2022.

7. Dagnachew AG, Hof AF, Roelfsema MR, van Vuuren DP. Actors and governance in the transition toward universal electricity access in Sub-Saharan Africa. Energy Policy 2020; 143: 111572.

8. Ndiaye A, Kébé CMF, Ndiaye PA. Impact of dust on the photovoltaic (PV) modules characteristics after an exposition year in Sahelian environment: The case of Senegal Correction of capability indices taking into account measurement errors View project Publications Prof. Papa Alioune NDIAYE, CIFRES-ESP Dakar View project. 2013.

9. PV magazine. https://www.pv-magazine.com/2021/10/11/10-gw-desert-to-power-pvinitiative-picks-up-150-million-in-funding/. 10 GW Desert to Power PV initiative 2021.

10. Power Africa. https://powerafrica.medium.com/supporting-the-expansion-of-solar-powerin-west-africa-c0730577fd3f. 2022.

11. Institute of Energy and Climate Research Techno-economic Systems Analysis (IEK-3). Africa h2 atlas. 2023.

12. Bhandari R. Green hydrogen production potential in West Africa – Case of Niger. Renew Energy 2022; 196: 800–811.

13. Hussain A, Batra A, Pachauri R. An experimental study on effect of dust on power loss in solar photovoltaic module. Renew Wind Water Sol 2017; 4.

14. Al-Addous M, Dalala Z, Alawneh F, Class CB. Modeling and quantifying dust accumulation impact on PV module performance. Solar Energy 2019; 194: 86–102.

15. Abuzaid H, Awad M, Shamayleh A. Impact of dust accumulation on photovoltaic panels: a review paper. International Journal of Sustainable Engineering 2022; 15: 264–285.

16. Ilse K, Micheli L, Figgis BW *et al.* Techno-Economic Assessment of Soiling Losses and Mitigation Strategies for Solar Power Generation. Joule 2019; 3: 2303–2321.

17. Perraki V. Temperature Dependence on the Photovoltaic Properties of Selected Thin-Film Modules. International Journal of Renewable and Sustainable Energy 2013; 2: 140.

18. Seidlitz HK, Thiel S, Krins A, Mayer H. Solar radiation at the Earth's surface. In: 2001: 705–738.

19. Ibrahim KA, Gyuk PM, Aliyu S. The effect of solar irradiation on solar cells. Science World Journal 14: 2019.

20. Tang X, Quan Z, Zhao Y. Experimental Investigation of Solar Panel Cooling by a Novel Micro Heat Pipe Array. Energy Power Eng 2010; 02: 171–174.

21. del Cueto JA. Comparison of energy production and performance from flat-plate photovoltaic module technologies deployed at fixed tilt. Conference Record of the TwentyNinth IEEE Photovoltaic Specialists Conference, 2002., IEEE, 1523–1526.

22. Krauter S, Araújo RG, Schroer S *et al.* Combined photovoltaic and solar thermal systems for facade integration and building insulation. Solar Energy 1999; 67: 239–248.

23. E. Skoplaki, A. G. Boudouvis, J. A. Palyvos, A simple correlation for the operating temperature of photovoltaic modules of arbitrary mounting, Sol. Energy Mater. Sol. Cells. 92 (2008) 1393–1402.

24. Schwingshackl C, Petitta M, Wagner JE et al. Wind effect on PV module temperature: Analysis of different techniques for an accurate estimation. Energy Procedia, Elsevier Ltd 2013, 77–86.

25. Effects-of-Dust-on-the-Performance-of-PV-Panels. Shaharin A Sulaiman, Haizatul H Hussain, Nik Siti H Nik Leh, and Mohd S I Razali 2011; 588–593.

26. Ghoneim, A.Y.A. and Al-Hasan, A. (2005) A New Correlation between Photovoltaic Panel's Efficiency and Amount of Sand Dust Accumulated on Their Surface. International Journal of Sustainable Energy, 24, 187-197.

27. Sulaiman SA, Singh AK, Mokhtar MMM, Bou-Rabee MA. Influence of dirt accumulation on performance of PV panels. Energy Procedia, Elsevier Ltd 2014, 50–56.

28. Bonkaney A, Madougou S, Adamou R. Impacts of Cloud Cover and Dust on the Performance of Photovoltaic Module in Niamey. Journal of Renewable Energy 2017; 2017: 1–8.

29. Dajuma A, Yahaya S, Touré S *et al.* Sensitivity of Solar Photovoltaic Panel Efficiency to Weather and Dust over West Africa: Comparative Experimental Study between Niamey (Niger) and Abidjan (C d'Ivoire). Computational Water, Energy, and Environmental Engineering 2016; 05: 123–147.

30. Ndiaye A, Kébé CMF, Ndiaye PA, Charki A, Kobi A, Sambou V. Impact of dust on the photovoltaic (PV) modules characteristics after an exposition year in Sahelian

environment: The case of Senegal. International Journal of Physical Sciences Full Length Research Paper 2013; 8: 1166–1173.

31. Sheila D, Simiyu N. Optimal Cleaning Strategy for Large Scale Solar Photovoltaic Array Considering Non-Uniform Dust Deposition. 2020.

32. Experimental Evaluation of the Effect of Inclination and Dust Deposition on Production Capacity of Photovoltaic Installations in West African Nations: Case Study in Mali Drame. Iranian Journal of Energy and Environment 2018; 9.

33. Chanchangi YN, Ghosh A, Sundaram S, Mallick TK. Dust and PV Performance in Nigeria: A review. Renewable and Sustainable Energy Reviews 2020; 121: 109704.

34. Henry Biwole P, Eclachec P, Kuznik F, Biwole P, Eclache P, Kuznik F. Phase-change materials to improve solar panel's performance Phase-change materials to improve solar panel's performance F b buoyancy force from Boussinesq approximation N.m-3 g gravitational constant m.s-2 outdoor convection heat transfer coefficient Wm-2 K-1 h indoor convection heat transfer coefficient Wm-2 K-1. Energy Build 2013; 62.

35. E. Cuce and P. M. Cuce, "Improving thermodynamic performance parameters of silicon photovoltaic cells via air cooling," International Journal of Ambient Energy, vol. 35, no. 4, pp. 193–199, 2014

36. Y. Indartono, S. Prakoso, A. Suwono, I. Zaini, and B. Fernaldi, "Simulation and experimental study on effect of phase change material thickness to reduce temperature of photovoltaic panel," in IOP Conference Series: Materials Science and Engineering, vol. 88, no. 1. IOP Publishing, 2015, p. 012049.

37. Abdolzadeh M, Ameri M. Improving the effectiveness of a photovoltaic water pumping system by spraying water over the front of photovoltaic cells. Renew Energy 2009; 34: 91– 96.

38. Moharram KA, Abd-Elhady MS, Kandil HA, El-Sherif H. Enhancing the performance of photovoltaic panels by water cooling. Ain Shams Engineering Journal 2013; 4.

39. Himanshu Sainthiya and Narendra S. Beniwal. Different Types of Cooling Systems Used in Photovoltaic Module Solar System: Conference Paper · March 2017; 878: 1500–1506.

40. Fathi M, Abderrezek M, Grana P. Technical and economic assessment of cleaning protocol for photovoltaic power plants: Case of Algerian Sahara sites. Solar Energy 2017; 147: 358–367.

41. Alamri HR, Rezk H, Abd-Elbary H, Ziedan HA, Elnozahy A. Experimental Investigation to Improve the Energy Efficiency of Solar PV Panels Using Hydrophobic SiO2 Nanomaterial. Coatings 2020; 10: 503.

42. Lubbe F, Rongé J, Bosserez T, Martens JA. Golden hydrogen. Curr Opin Green Sustain Chem 2023; 39: 100732.

43. Wang M, Wang G, Sun Z, Zhang Y, Xu D. Review of renewable energy-based hydrogen production processes for sustainable energy innovation. Global Energy Interconnection 2019; 2: 436–443.

44. Patent Office E, International Renewable Energy Agency the. Innovation trends in electrolyzers for hydrogen production: Patent insight report.

45. APA. IRENA, I. (2020). Green hydrogen cost reduction: scaling up electrolyzers to meet the 1.5 C climate goal. Abu Dhabi: International Renewable Energy Agency.

46. CertifHy, CertifHy - Developing a European Framework for the generation of guarantees of origin for green hydrogen, 2016, https://www.certifhy.eu/images/media/files/CertifHy__ definition_outcome_and_scope_LCA_analysis...

47. Terlouw T, Bauer C, McKenna R, Mazzotti M. Large-scale hydrogen production via water electrolysis: a techno-economic and environmental assessment. Energy Environ Sci 2022; 15: 3583–3602.

48. Shiva Kumar S, Lim H. An overview of water electrolysis technologies for green hydrogen production. Energy Reports 8 2022 13793–13813.

49. Frangopoulos CA. Recent developments and trends in optimization of energy systems. Energy 2018; 164: 1011–1020.

50. Papoulias SA, Grossmann IE. A structural optimization approach in process synthesis—I. Comput Chem Eng 1983; 7: 695–706.

51. Amer M, Namaane A, M'Sirdi NK. Optimization of Hybrid Renewable Energy Systems (HRES) Using PSO for Cost Reduction. Energy Procedia 2013; 42: 318–327.

52. Renewable Energy Agency I. Renewables Readiness Assessment: Niger. 2013.

53. Langiu M, Shu DY, Baader FJ *et al.* COMANDO: A Next-Generation Open-Source Framework for Energy Systems Optimization. Comput Chem Eng 2021; 152.

54. Meurer A, Smith CP, Paprocki M *et al.* SymPy: symbolic computing in Python. PeerJ Comput Sci 2017; 3: e103. Mattei M, Notton G, Cristofari C, Muselli M, Poggi P. Calculation of the polycrystalline PV module temperature using a simple method of energy balance. Renew Energy 2006; 31: 553–567.

55. Sainthiya H, Beniwal NS. Different types of cooling systems used in photovoltaic module solarystem: A review. Proceedings of the 2017 International Conference on Wireless. Communications, Signal Processing and Networking, WiSPNET 2017, Institute of Electrical and Electronics Engineers Inc. 2018, 1500–1506.

56. Mattei M, Notton G, Cristofari C, Muselli M, Poggi P. Calculation of the polycrystalline PV module temperature using a simple method of energy balance. Renew Energy 2006; 31: 553–567.

57. Short W, Packey DJ, Holt T. A Manual for the Economic Evaluation of Energy Efficiency and Renewable Energy Technologies. 1995.

58. Millennium Challenge Corporation (MCC), Nancy Kim PIC and PA. Niger, most groundwater-rich country in the Sahel region Millennium Challenge Corporation (MCC). 2023.

59. Basrawi MF, Anuar MNAF, Ibrahim TK, Razak AA. Experimental analysis on the effect of cooling surface area and flow rate for water-cooled photovoltaic module. IOP Conference Series: Materials Science and Engineering, Institute of Physics Publishing 2020.

60. Water treatment for Green Hydrogen. https://hydrogentechworld.com/water-treatment-forgreen-hydrogen-what-you-need-to-know.

61. Caldera U, Bogdanov D, Breyer C. Desalination Costs Using Renewable Energy Technologies. In: Renewable Energy Powered Desalination Handbook. Elsevier, 2018: 287–329

62. Gurobi Optimization, LLC. Gurobi Optimizer Reference Manual. 2021.

63. Sharma V, Chandel SS. Performance and degradation analysis for long-term reliability of solar photovoltaic systems: A review. Renewable and Sustainable Energy Reviews 2013; 27: 753–767.

64. https://www.renewables.ninja/. 2019.

65. Pfenninger S, Staffell I. Long-term patterns of European PV output using 30 years of validated hourly reanalysis and satellite data. Energy 2016; 114: 1251–1265.

66. Niger: Request for a Three-Year Arrangement Under the Extended Credit Facility-Press Release; Staff Report; and Statement by the Executive Director for Niger; IMF Country Report No. 21/271; November 19, 2021. 2021.

67. Ramasamy V, Margolis R. Floating Photovoltaic System Cost Benchmark: Q1. Installations on Artificial Water Bodies. 2021.

68. Fathi M, Abderrezek M, Grana P. Technical and economic assessment of cleaning protocol for photovoltaic power plants: Case of Algerian Sahara sites. Solar Energy 2017; 147: 358–367.

69. Stehly T, Duffy P. 2020 Cost of Wind Energy Review, National Renewable Energy Laboratory. 2020.

70. Hadipour A, Rajabi Zargarabadi M, Rashidi S. An efficient pulsed-spray water cooling system for photovoltaic panels: Experimental study and cost analysis. Renew Energy 2021; 164: 867–875.

71. Mukelabai MD, Gillard JM, Patchigolla K. A novel integration of a green power-to ammonia to power system: Reversible solid oxide fuel cell for hydrogen and power production coupled with an ammonia synthesis unit. Int J Hydrogen Energy 2021; 46: 18546–18556.

72. Seitz M, von Storch H, Nechache A, Bauer D. Techno-economic design of a solid oxide electrolysis system with solar thermal steam supply and thermal energy storage for the generation of renewable hydrogen. Int J Hydrogen Energy 2017; 42: 26192–26202.

73. IEA. Countries Energy system. Analysis Energy system Low-Emission Fuels Electrolysers Electrolysers. 10 July 2023.

74. Gigawatt green hydrogen plant. 2020. https://ispt.eu/projects/hydrohub-gigawatt/

75. Dias V, Pochet M, Contino F, Jeanmart H. Energy and Economic Costs of Chemical Storage. Front Mech Eng 2020; 6.

76. ONEL Transforming Energy. Annual Technology Baseline, Utility-Scale Battery Storage.

77. Elberry AM, Thakur J, Santasalo-Aarnio A, Larmi M. Large-scale compressed hydrogen storage as part of renewable electricity storage systems. International Journal of Hydrogen Energy 46 2021 15671–15690.

78. Alliance SAHEL. Presentations-table-ronde-electricite-Niger-jour1-1. Presentation de la 1iere Table ronde Alliance SAHEL 2020

79. Salihou Djari MM, Stoleriu CC, Saley MB, Mihu-Pintilie A, Romanescu G. Groundwater quality analysis in Warm Semi-Arid climate of Sahel countries: Tillabéri Region, Niger. Carpathian Journal of Earth and Environmental Sciences 2018; 13: 277–290.